NTNU – Trondheim
Norwegian University of
Science and Technology

Hydraulic Fracturing for Enhanced Geothermal Systems

Mats Rongved

Petroleum Geoscience and Engineering
Submission date: June 2015
Supervisor: Rune Martin Holt, IPT
Co-supervisor: Alexandre Lavrov, SINTEF
Idar Larsen, SINTEF

Norwegian University of Science and Technology
Department of Petroleum Engineering and Applied Geophysics

Abstract

Finding new energy sources to provide base load electricity supply on a global scale is of increasing importance. Enhanced Geothermal Systems (EGS) has been identified as capable of playing an important role in the future of the energy market. The normally overlooked energy source has a great resource base, but faces challenges in order to become a serious energy alternative on a global scale. The main focus of this thesis is to investigate the properties demanded of effective fracture networks for EGS and the way forward to ensure our ability to consistently stimulate them. To stimulate a swarm of parallel propagating fractures is identified as a way forward. Dike swarms, which are naturally occurring parallel fracture swarms, is an area that can provide valuable information to stimulate parallel hydraulic fractures over long distances. A numerical study was carried out to investigate the effect of the stress regime and of injection point distance on multiple fracture interaction. It was found that the stress regime severely affect fracture interaction, and the ability of fractures to propagate parallel is seriously reduced in low contrast stress regimes. This indicates that it is important to take the stress regime into account when designing multi stage fracture jobs. It was also found that the ability of fractures to extend for long distances is reduced if the spacing between injection points become too small.

Sammendrag
Å finne alternative kilder til å dekke verdens energibehov blir stadig viktigere. En het kandidat i denne sammenhengen er såkalt «Enhanced Geothermal Systems» (EGS) eller konstruerte geotermiske systemer. Denne vanligvis oversette energikilden, har en stor ressursbase, men står foran flere utfordringer før den kan bli et seriøst alternativ på global plan. Hovedfokuset til denne mastergraden har vært å utforske egenskapene som er krevd av et effektivt sprekknettverk for EGS, og hvordan man konsekvent kan stimulere dannelsen av disse. Å stimulere dannelsen av en sverm av parallelle sprekker er blitt identifisert som en mulig vei fremover. Studie av gangsvermer, som er svermer av naturlige parallelle sprekker, kan bidra med viktig informasjon om hvordan man kan stimulere dannelsen av hydrauliske parallelle sprekker over lange avstander. Et numerisk studie er i den sammenheng blitt gjennomført. Her har det blitt undersøkt hvordan spenningsforhold og avstanden mellom injeksjonspunkt påvirker interaksjonene mellom sprekkene. Det har blitt funnet at spenningsforholdet påvirker sprekkinteraksjonen i stor grad, og at evnen sprekkene har til å propagere parallelt blir kraftig redusert hvis spenningskontrasten er liten. Dette indikerer at det er viktig å ta hensyn til spenningsforholdet når man planlegger en flerstegs frakturerings jobb. Videre har det blitt funnet at sprekkenes evne til å propagere over lange avstander blir redusert hvis avstanden mellom injeksjonspunktene blir for kort.

Acknowledgements

Here is a list of the people I would like to thank for help and support during the work on my master thesis. An extra thank to my supervisors for excellent guidance.

- Rune Holt
- Alexandre Lavrov
- Idar Larsen
- Knut Sverdrup
- Pappa
- Family and friends

Contents

List of Figures

List of Tables

Chapter 1

Introduction

Base load power sources are an important foundation for modern society. They are necessary for the functionality of our daily doings, and also key assets in the increase in living standard across the globe. The increasing world population combined with the challenges related to climate change and other environmental impacts, pose several challenges for the energy production industry [1]. Over the last 100 years petroleum resources have been a major contributor to the energy market, but we are now facing a decline in resources and the environmental impacts are possibly severe [1]. It is therefore of great importance to start looking for new ways of establishing secure energy production sources on a global scale. Geothermal energy has been much overlooked in this context [2]. It is normally only related to the extraction of heat from conventional resources in limited locations, such as Iceland and Japan. Recent studies show that the potential of so called Enhanced Geothermal Systems (EGS) can play an important role in the future of the energy market [2]. The resource base is large, and they share several challenges with the petroleum industry, facilitating for adaptation of existing techniques from an industry with a high technology development [3]. EGS is a way of mining heat from unconventional resources commonly found around the world, by drilling to great depths, and stimulating the rock in order to create an effective system. Both the stimulation and the drilling process poses several technological challenges that need to be overcome in order for EGS to be commercially attractive. These challenges are mostly related to technologies that already exist and are in need of improvement, more than realising new ones [2]. The main constraint in making EGS a base load power source on a global scale, has been identified as being able to consistently stimulate desirable fracture networks [2]. Such a network is able to ensure a high daily capacity as well as a long field life, in order to make a project economically viable. The main focus of this thesis will be to investigate the properties demanded of these fractures and the way forward to ensure our ability to stimulate them in a consistent manner.

Chapter 2 is a background study of hydraulic fracture stimulation for EGS. Geothermal energy and the different types of heat mining systems are introduced in section 2.1. This section is taken as a whole, with small modifications, from the project thesis by Rongved[3]. Chapter 2.2 introduces the governing trends of hydraulic fractures with some secondary effects, before discussing problems faced at previous EGS projects, and presenting a way forward for EGS fracture networks. The subsection "Hydraulic fracture stimulation for EGS" of section 2.2, is partly inspired by Rongved[3], and contains some elements from this project thesis. In section 2.3, dike swarms, their relevance for EGS, and possible lessons learnt from the area are discussed. Numerical modelling as a tool to investigate hydraulic fractures, with a focus on the Modified Discrete Element coupled with Tough2, is introduced in section 2.4. MDEM and Tough2 are also the methods used for the numerical simulations in this thesis. Chapter 3 introduces the numerical scheme for numerical investigations, including a physical description of the reservoir and simulation design, before describing the numerical approximations to the design. The relevant results are presented and discussed in chapter 4 and 5 respectively. Further work is introduced in chapter 6 before the thesis is concluded in chapter 7.

Chapter 2

Introduction to Enhanced Geothermal Systems, potential and complications

2.1 Geothermal energy

Heat in the crust

Thermal energy found within the earth has primarily been formed as a result of two major processes; heat created during the formation of the earth, and new thermal energy created through radio active decay of mainly three isotopes: thorium, uranium and potassium[4]. In the crust heat is stored and transferred through rock structures, and through fluids if they are present. When fluids are present, they are stored in small pores, fractures, and other open spaces in between the rock matrix. Heat transfer within the rock matrix happens through a process called conduction, which is transfer of kinetic energy between molecules, and which does not involve movement of mass. If there is communication between the pores, flow is possible, allowing a transfer of mass as well. This type of heat transfer is called convection, and involves the transfer of a heated mass from one place to another. When looking at the crust, convection is generally a more effective method of heat transfer than conduction, as rocks are very poor thermal conductors[4]. Large fractions of the crust consist of impermeable rock, however, and do not allow fluid flow. Convection is a rarity in most places. The rock's conductivity, and the amount of heat formed from radio active decay within the rock mass, normally set the foundation for the thermal gradient. This gradient defines how much the temperature increases with depth, averaging at approximately 30 degrees Celsius per kilometre in crust. In some areas much higher values can be reached[4]. Often younger rock formations have steeper thermal gradients, and the highest values found are in volcanic regions or at tectonic borders.

Thermal systems

From a geothermal engineering point of view, thermal systems are established to extract heat from the earth. Geological conditions in the reachable crust around the world vary greatly, and as a result the approach to design and exploit geothermal heat varies too. The ideal situation is a large, porous, highly permeable reservoir, located at shallow depths and at very high temperatures. Reservoirs with porous and permeable rock masses similar to typical hydrocarbon reservoirs are common, but the high temperatures seldom occur except in areas with volcanic heat sources close to the reservoir. A more common condition for a thermal system is close to impermeable, hard, igneous rock at great depth. This poses several challenges for the developer to make it economically attractive. See figure 2.1 for a comparison of the different systems. In order to extract thermal energy from these unconventional reservoirs, deep wells must be drilled at difficult conditions. In addition to this, an effective network of fractures must be stimulated between the injection and production well. After achieving a good circulation network, cold water can be pumped into the system, gaining heat from the rock mass on the way. When the heated water reappears at the surface, the heat is extracted and cold water is pumped back down. Establishing a good fracture network in a large volume of rock while sustaining good communication can be very challenging, and with the addition of high drilling costs, Enhanced Geothermal Systems face several challenges in order to be realised as a serious energy alternative globally.

Unconventional reservoirs

The essence of EGS is that cold water (we assume water, although other substances may be possible alternatives) is injected into the reservoir through an injection well, after which it flows through cracks and fractures, obtains heat from the reservoir rock, and finally flows back to the surface through a production well. At the surface, heat is transformed to electric energy, and cold water is re-injected in order to obtain more heat. See figure 2.2 for an EGS system overview. The energy efficiency of the system is dependent on the amount of heat obtained by the water on its

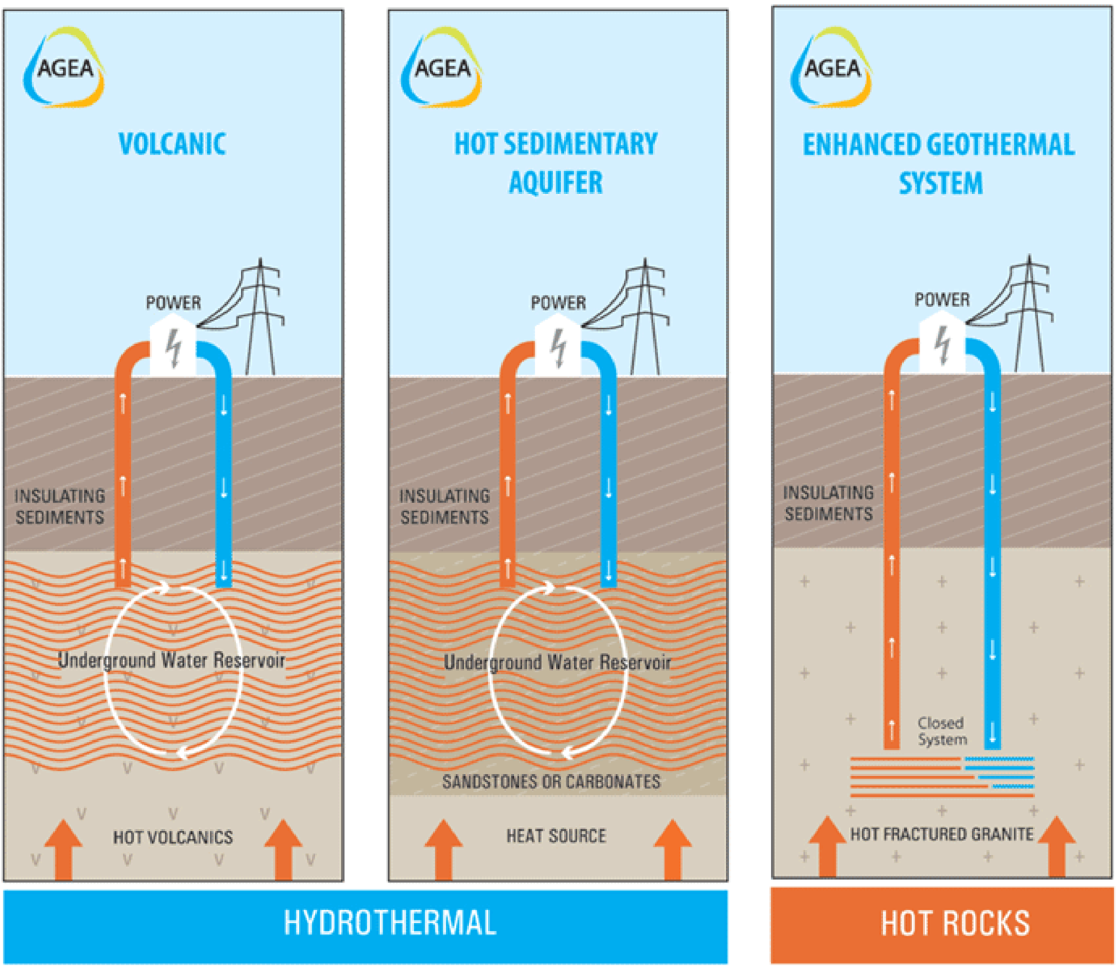

Figure 2.1: Geothermal systems. From left to right are diagrams for volcanic, conventional and unconventional systems. This thesis is mainly concerned with EGS, shown in the right image. Image copyright AGEA.

path from the injection point to production point. If a high flow rate is maintained, and high temperatures are achieved in the production fluid at the same time, large amounts of energy can be extracted from the reservoir. For the water to heat up quickly, the ratio of rock surface area to water volume flow must be high. In other words, a flow path consisting of many small cracks is better than a few large ones. Because convection is a much more effective way to transfer heat than conduction, it is essential that the water reaches as big a part of the reservoir volume as possible. In this manner, heat can be extracted more evenly from the reservoir. This results in a longer field life, and exposes the water to a greater total heat source, maximizing daily production capacity. In order to achieve an efficient EGS it is therefore necessary that the fracture network has a high surface to volume ratio, extends to a big part of the reservoir and has good communication between the injection and production well.

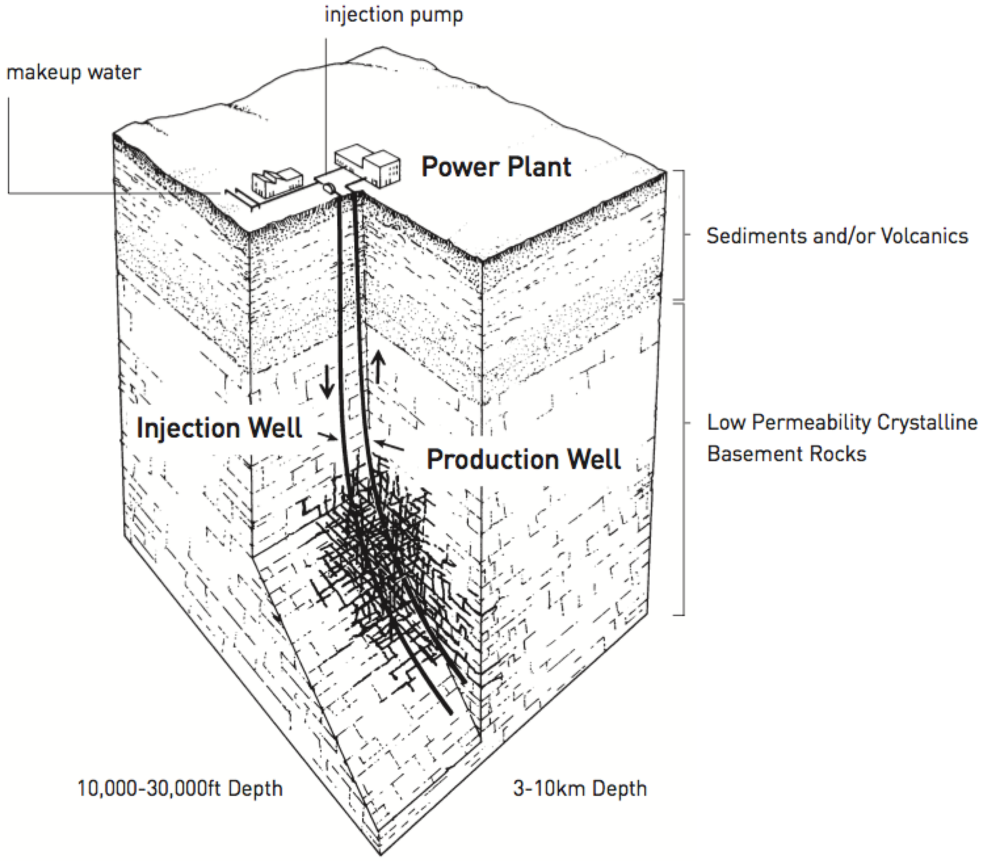

Figure 2.2: Schematic of a conceptual two-well EGS in hot rock in a low-permeability crystalline basement formation. Image taken from Tester et al. (2006)[2]

Specifications of a good geothermal system

Unconventional geothermal reservoirs are usually found at great depths in the crystalline basement, a rock mass which consists of various types of igneous rock. Although rock masses at these depths contain small fissures and cracks and are not completely impermeable, they do tend to have very bad connectivity between cracks[5]. In order to achieve the desired permeability and connectivity stimulation is needed. Stimulation has been successfully implemented for decades in the petroleum industry through a method called hydraulic fracturing. This is a mechanism used to maximize production rate and total amount of recoverable resources. Fracturing is normally done by pumping a fracturing fluid at a high rate and pressure into the desired zone. This causes existing fractures and discontinuities to extend and allows new ones to form and propagate[6]. Many properties affect the propagation and extensiveness of these fractures. And with the depths at which these reservoirs are located, makes it very difficult to obtain accurate information, design good models and achieve the desired results.

Tester et al. (2006)[2] concluded in their extensive review of geothermal energy resources in USA:

" At this point the main constraint is creating sufficient connectivity within the injection and production well system in the stimulated region of the EGS reservoir and allow for high per-well production rates without reducing reservoir life by rapid cooling the most essential challenges to overcome are related to reservoir stimulation, accurately predicting and modelling rock mass reaction to stimulation, facilitating for a good design and consistent development of effective EGS".

In other words, the biggest constraint in commercializing EGS lies within the field of reservoir technology, and finding a stimulation design that will consistently be able to produce effective EGS.

2.2 Hydraulic fracturing

For EGS, the primary role of hydraulic fracturing is to establish a satisfactory fracture network between a production well and an injection well. Hydraulic fracturing has already been a valuable technique in several industries to stimulate reservoir rock, with the objective varying from increased oil and gas recovery in the petroleum business to establishing a circulation network in geothermal industry. There are, however, two main goals of fracturing that are common across industries. The first is to reach the desired volume of rock, and the second to ensure satisfactory connectivity within the fracture network. These two goals can at times be difficult to achieve, and doing so is an important challenge to better the understanding of how untouched rock mass behaves to stimulation.

Hydraulic fracturing can be simplified into a process that happens when the fluid pressure at a given point in earth exceeds the least of the principal stresses[7]. This criterion can be met both naturally or artificially, either through an increase in fluid pressure or a decrease in the stress. Examples of naturally occurring hydraulic fractures are basaltic dikes, hydro thermal veins and up-welling of magma[7]. Some of these phenomena can be observed even after they have occurred, and can produce valuable information to help us understand fracture propagation in the crust better. Dike swarms are a naturally occurring swarm of parallel propagating dikes, a phenomenon of special interest for EGS which will be described in greater detail in chapter 2.3.

Initiation

Industrial hydraulic fractures are normally initiated by drilling a well into the reservoir, and increasing the pressure in a closed part of the well until the bore wall fails. An approximation for the well pressure need for the bore wall to fail is [8]

$$P_{w,\max}^{\text{Frac}} = 2\sigma_h - p_f + T_0. \tag{2.1}$$

Here, σ_h is the least principal stress, p_f is the pore pressure, and T_0 is the tensile strength of the rock. When the failure criterion is met, the bore wall fails and a fracture is initiated.

One wing of fracture is often initiated first, and when the pressure in the well becomes high enough to reach the failure criterion for a second wing, a new fracture is initiated [9], creating a so called bi-wing fracture as depicted in figure 2.3. There is a general consensus that the stress regime governs the direction in which the fractures are initiated, and later propagate. For initiation, this assumes a perfectly even bore wall, and the actual case is that there are often small fractures or weaknesses on the wall, causing the fractures to be initiated in other directions. Fractures initiated due to weaknesses in the bore wall will tend to align themselves with the direction governed by the stress field as they propagate [10]. In figure 2.3, a bi-wing fracture is initiated in a direction deviating from the preferred path, but gradually bends towards the maximum stress, and normal to the minimum stress. According to Zhang et al. [10], fracture initiation in a direction not aligned with the stress field can cause fracture tortuosity near the well bore and ultimately lead to a complex fracture network. This can in turn cause an early arrestment of the fracture growth, lead to leak-offs, and thus hinder the fractures from propagating the desired distance. In reservoirs that contain natural discontinuities, near-wellbore tortuosity can have a serious negative effect on the success of the stimulation treatments [10]. Several approaches exists to reduce near-wellbore tortuosity. One option is to increase the viscosity and the injection rate of the fluid, which has been shown to be quite effective [11]. This method can, however, lead to higher costs as additives to the injection fluid are necessary. Another approach is to use perforations aligned with the maximum stress, as fractures tend to stay in the direction they are initiated, and recent field examples show that this can be an effective technique to reduce treating pressure and pre-mature screenout [12,13].

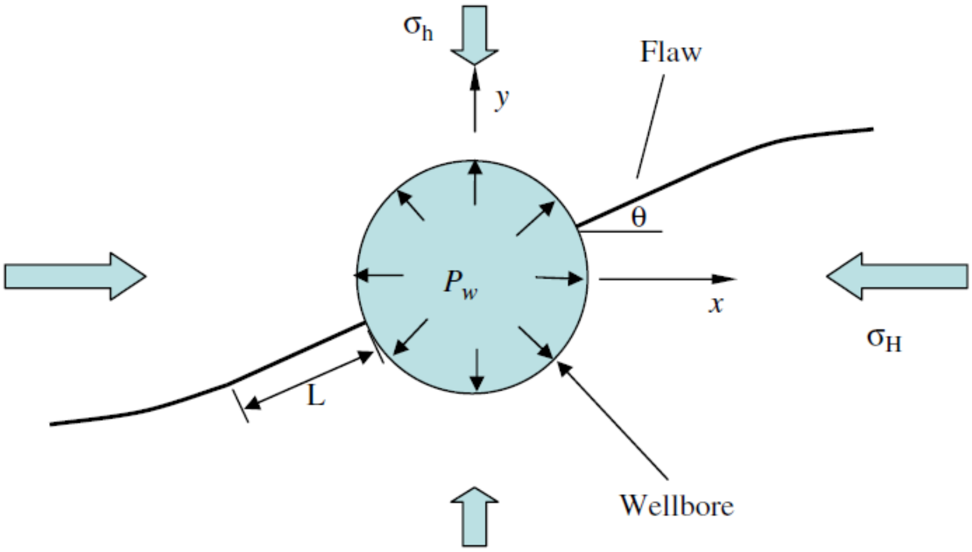

Figure 2.3: An illustration of a bi-wing fracture initiated from a well at a direction deviating from the preferred path given the stress field, before bending normal to the minimum stress. Image taken from Zhang et al.[10]

Hydraulic propagation

Looking at an ideal homogeneous rock, fractures tend to propagate in a direction normal to the least principal stress. This can be explained by a principle of work minimization: natural processes minimize the work needed for the process to occur[7]. A fracture does work by expanding the volume which it occupies. For the fracture to propagate it must separate the rock matrix at the tip of the fracture. Looking only at the stress regime, this mainly means overcoming the stress normal to the fractures direction. The fracture propagation must hence be normal to the least principal stress , denoted as σ_3. For the pre-existing fracture to expand its width it also has to overcome σ_3, but due to the geometry of the fracture it will have to partially open towards other, larger stress components. In addition to this, the expansion of the fracture will compress the rock matrix and, as a result, increase σ_3. Thus, it becomes harder for the fracture to expand the wider it grows. This simplification explains why fractures tend to be long and thin rather than short and thick[7]. Figure 2.4 illustrates a penny-shaped fracture propagating from a well, in addition to the fluid pressure distribution at the fracture tip. A simplified criterion for the fractures propagation can be given as

$$\sigma - p_f < T_0, \tag{2.2}$$

stating that the fluid pressure p_f must overcome the acting stress σ, as well as the acting tensile strength T_0 at the tip. The fracture propagation is thus dependent on both the fluid flow in fractures and on the behaviour of *in situ* rock mass. As mentioned, the stress regime is the governing factor for fracture behaviour, but several other secondary effects can severely affect the fracture's local behaviour and limit our ability to deliver the desired fluid pressure to the tip. One of these effects, is the tensile strength of the rock, i.e. the rock's ability to resist failure. For the rock to break, the pressure must overcome the tensile strength of the rock. This is normally substantially lower than the effect of the stress regime, but on a small scale it can cause deviations in the propagation direction.

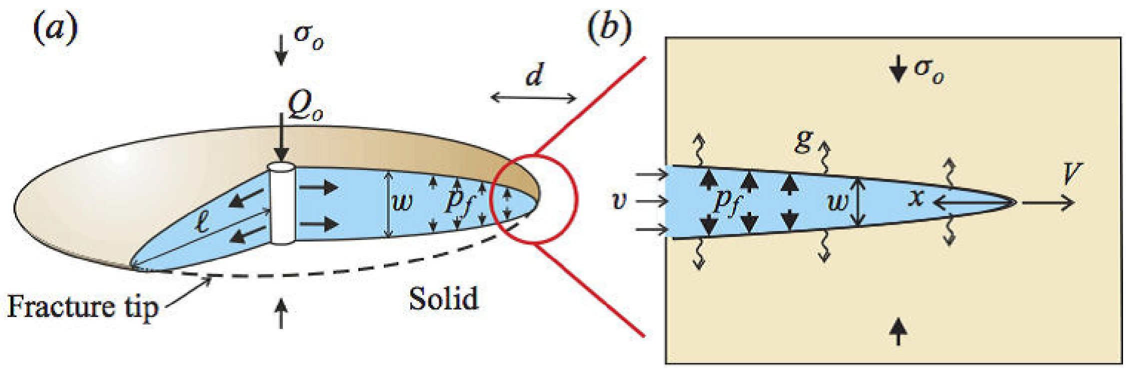

Figure 2.4: An illustration of a penny-shaped fracture, with axi-symmetric flow. Image taken from Charles Fairhurst[14]

Other effects

The crust has been exposed to alterations and changes over millions of years, such as stress from tectonic movement, mineralogy changes etc. These changes have caused heterogeneity in rock properties, stress zones and natural permeability. All these factors may affect the fracture behaviour, through deviations from the expected path, total arresting of the fracture and leak-offs. These effects may be crucial to predict in order to complete a successful fracturing job, as they can cause fractures to head off in undesired directions, or not propagate for the desired distance. This can result in poor production for a petroleum well, or a lack of communication in an EGS reservoir, and research points out that for accurate modelling of fracture propagation these secondary effects must be taken into account[14–20]. We normally only have access to a small core and limited seismic data, and are expected to define the properties for reservoirs up to a cubic kilometre. This makes it close to impossible to accurately define heterogeneity, and secondary effects will therefore be discussed based on the general effects they can have on fracture stimulation, and on measures to minimize these effects.

Natural permeability

The crust is highly heterogeneous and contains several geological discontinuities. These are phenomena such as faults, cracks and bedding planes. Discontinuities may change local parameters such as permeability, tensile strength and stress, and when a hydraulic fracture encounters such a zone, the impact of these parameter alterations might be big enough to cause a deviation from the direction it was previously propagating in[16,18]. With an already existing permeability in the natural crack and no need to overcome tensile strength, the natural crack might be extended for a while, as it demands less work than for the fracture to continue on its original path. After a while the fracture might break of from the new direction back to the old one, or it might arrest at a point and the fracture can be reactivated at an earlier stage. This type of behaviour can cause a very complex fracture network, where natural permeability is activated and arrested, or becomes part of the main fracture path. An example of this type of behaviour can be seen in figure 2.5. With a more complex network the number of small cracks increases. This may cause severe leak offs, resulting in high demand on pump capacity or even arresting of the fracture propagation in the desired direction[16,18]. The effect of material property variations is lower when the stress contrasts are big, but can significantly affect the overall geometry of the fracture networks[16]. Measures to try and minimize the effect of complexity can be high viscosity fluids[10] and drilling wells normal to the minimum principal stress[5].

Thermal effects

For geothermal reservoirs, which are typically very hot, and which are stimulated with a much cooler liquid, thermal effects arise. When a rock mass is cooled, a compaction occurs, and the horizontal stress might decrease. This can cause a fracture initiation to occur at a much lower pressure than expected. Perkins and Gonzales[15] developed a numerical model to calculate the effects of these cooled regions. For further improvements in accuracy of fracture modelling, thermal effects should be included, but we do not consider these effects in more detail in this thesis.

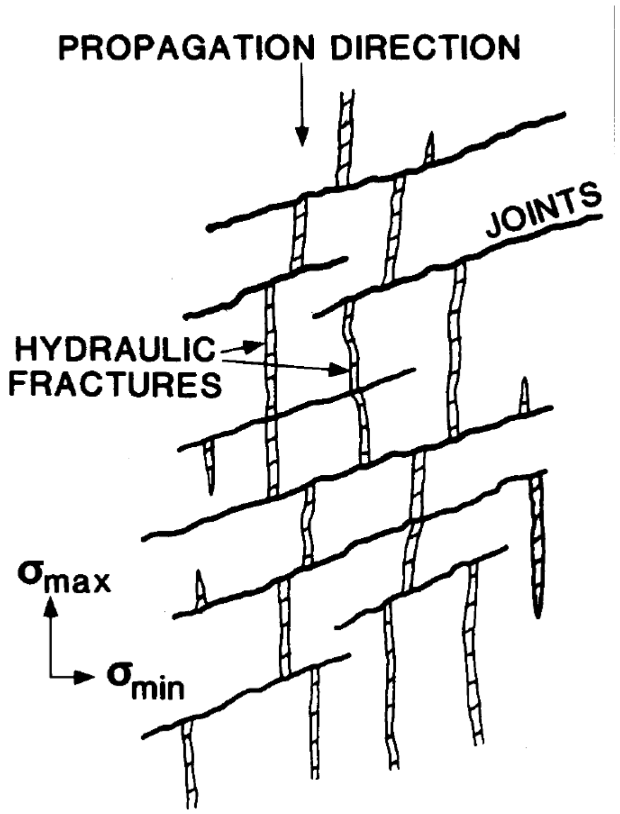

Figure 2.5: An illustration showing complex fracture propagation through a network of natural discontinuities. Image taken from Warpinski and Teufel [16]

Multiple fracture interaction

Multiple fracture stimulation jobs are a large part of the reason unconventional resources, such as shale gas, have been successfully exploited during recent years [21]. For EGS projects as well, multiple fractures initiated at a proximity to each other are necessary in order to achieve a satisfactory network [5]. Multiple fractures can be stimulated in series or during parallel injection. Fractures stimulated simultaneously can be defined as a fracture stage, and with several stages completed subsequently, we achieve a multi-stage fracturing job. As fractures propagate they take up a volume in the rock matrix and therefore affect their local surroundings. This is evident in the stress regime through an effect called stress shadowing [21]. A local change in the stress regime can cause fractures to deviate from the far stress field, and what the rig might believe is the preferred direction. It is therefore of great importance to understand how fractures alter the stress regime and in turn how they interact with each other when stimulated in the same area. In addition to fractures deviating from the preferred path, fracture interaction can cause merging of several fractures into one, limiting or even totally arresting a fracture's growth in a certain direction.

Because the crust is geologically complex, interactions between fractures are complicated. The effect of other factors on fracture propagation, such as natural discontinuities and rock heterogeneity, might increase if fractures are stimulated close to each other. Investigation of several governing factors, such as the effect of distance between injection points has be done in simplified conditions[21,22]. This implies some uncertainty, but is a starting point, identifying the effect of some of more governing factors such as stress regime and fracture distance. Figure 2.6 shows an illustration of an idealized multiple fracture propagation without interference, and how interference might affect the propagation.

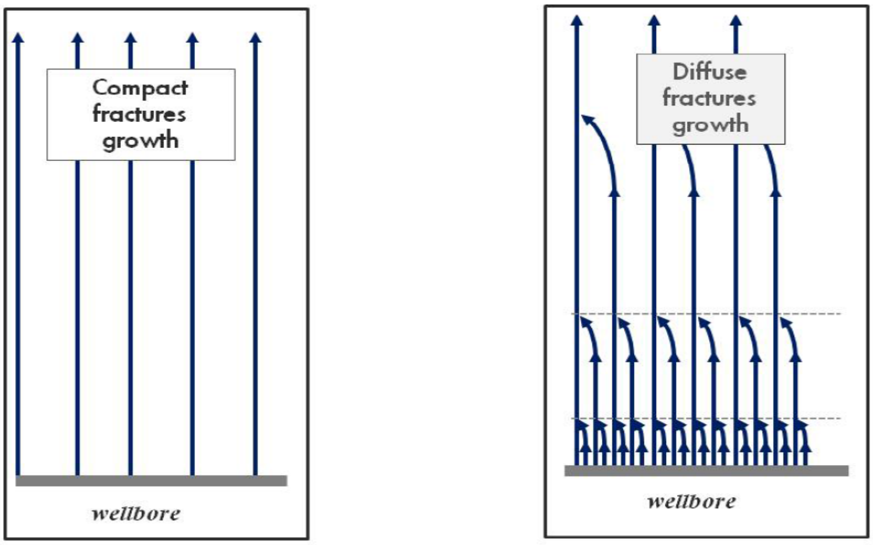

Figure 2.6: Illustrations of fractures propagating without interaction to the left, and possible propagation with interaction to the right. Image taken from Wong et al.[21]

Hydraulic fracture stimulation for EGS

Over the years several EGS projects have been conducted, but the technique is not mature enough to consistently produce economically viable base load electricity production[2]. Jung[5] carried out an extensive review of some of the most prominent EGS projects in order to investigate the way forward for EGS, going over the methods applied, results achieved and observations made. This section will be based on the projects reviewed there, and on some of the conclusions made.

All of the projects studied produced unsatisfactory results, and it was concluded that it was the underlying concept of rock mass behaviour that was misunderstood. Before the 1980s the general view of the crystalline basement considered it as a more or less intact and impermeable rock mass[5]. This lead the first approaches for EGS to create artificial flow paths from the production well to the injection well. The idea was that by drilling the wells parallel to the least principal stress and stimulating isolated bore hole sections, it would be possible to create a series of tensile fractures between the wells, similar to the right illustration in figure 2.7. This concept was initially applied at the Los Alamos with limited success. The failure was believed to be partly due to the reservoir fractures extending in unpredicted directions, caused by a shift in stress regime that was not anticipated[2]. After Los Alamos, all reviewed projects used a different underlying concept for designing the stimulation method. It was discovered that even down in the crystalline basement, the rock contained small fissures and natural fractures, and even though the natural permeability was very low, it was believed that it would be possible to extend and expand these natural discontinuities in order to establish a flow network for the geothermal energy production. The general idea was to stimulate a very long open bore hole with a massive water injection, and then drill a second well into this zone of believed enhanced permeability. An illustration of this concept can be seen in the left illustration in figure 2.7.

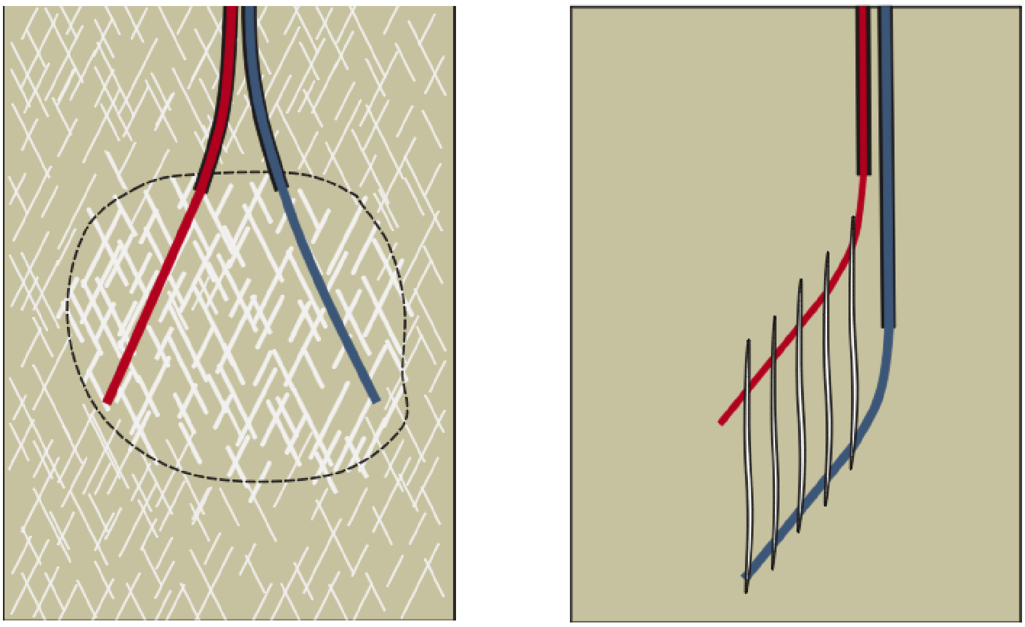

Figure 2.7: Comparison of early proposals for EGS fracturing. The left picture shows fracture stimulation through a long open bore hole, while the right depicts multi-scheme fracturing. Image taken from Reinhard Jung[5].

According to Jung, the underlying concept of attempting to extend natural fractures, is one of the major reasons for the subtle development in EGS efficiency. This is because the understanding of how fractures propagate through the natural discontinuities was wrong. Jung proposed that the granite cannot be looked at as a discontinuum on the small scale of joints, and the basic idea of the Coulomb failure criterion cannot be applied on this scale, but only on the scale of faults or fracture zones[5]. From the review it was found believable that even though many hundreds of natural fractures on the open well bore wall were stimulated, only one or very few fractures accounted for the large majority of fluid flow in the reservoir. An illustration of this effect from the Soultz project can be seen in figure 2.8.

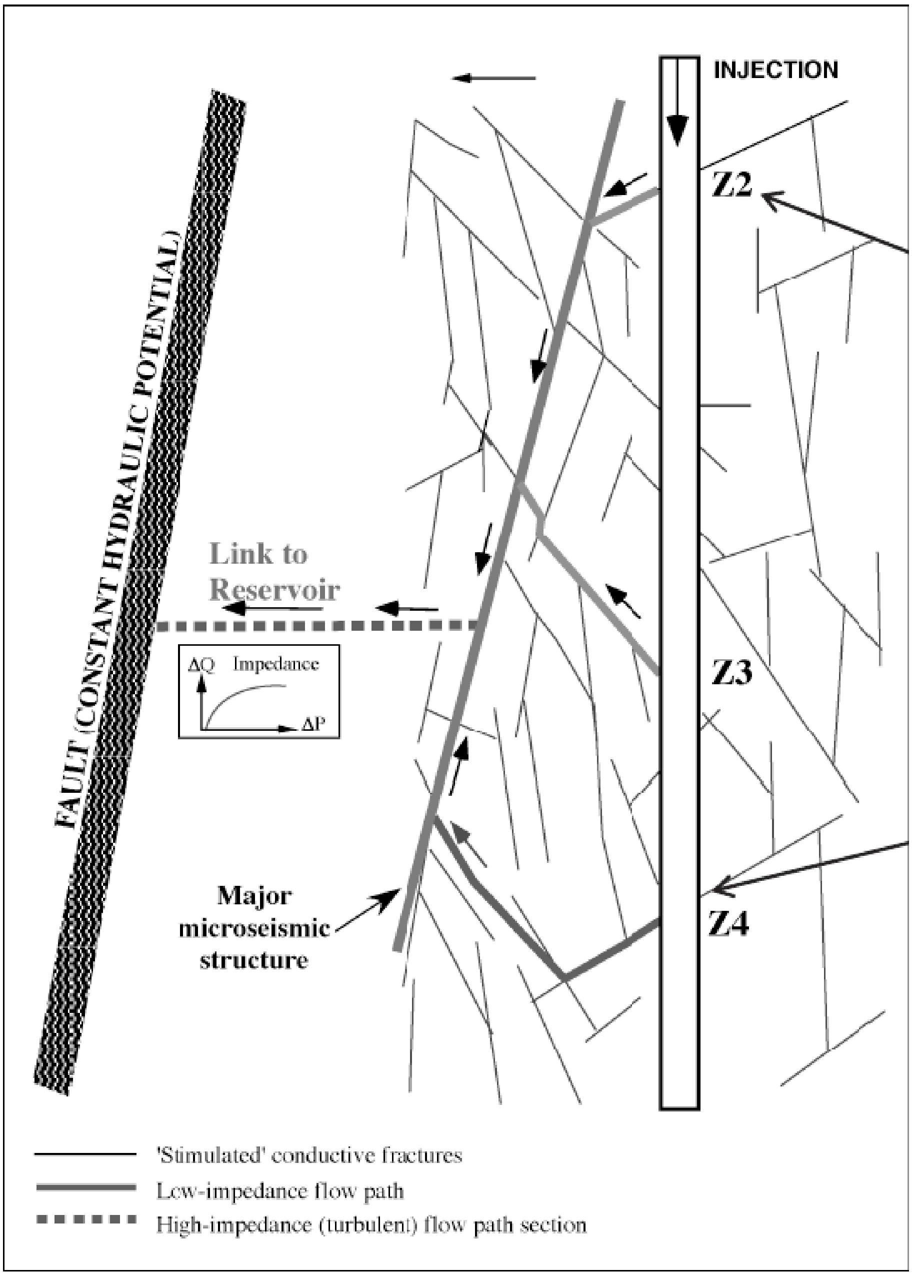

Figure 2.8: An illustrration from Soultz showing how many minor fractures merge into one large fracture containing most of the flow. Image taken from Reinhard Jung[5].

Since fractures were produced at pressures far below the minimum principal stress and normal tensile fracture models normally are not related to the intense seismicity of these events, Jung proposed wing cracks as a possible solution for the unpredicted behaviour of the fractures[5]. The proposal of a wing crack model is shown in figure 2.9. Wing cracks are believed to form when fractures of finite length fail under shear conditions. These cracks do not propagate along the fractures axis, but tend to migrate of around 70 degrees and gradually turn in the direction of maximum principal stress[23]. These wing cracks formed at the end of pre-existing cracks, with large volume to surface ratios, are an explanation to the unexpected and poor results for these projects[5]. Through this research, Jung states that the approach of trying to expand and extend the natural fractures and fissures into a suitable EGS fracture network will never be successful. Jung suggests that a

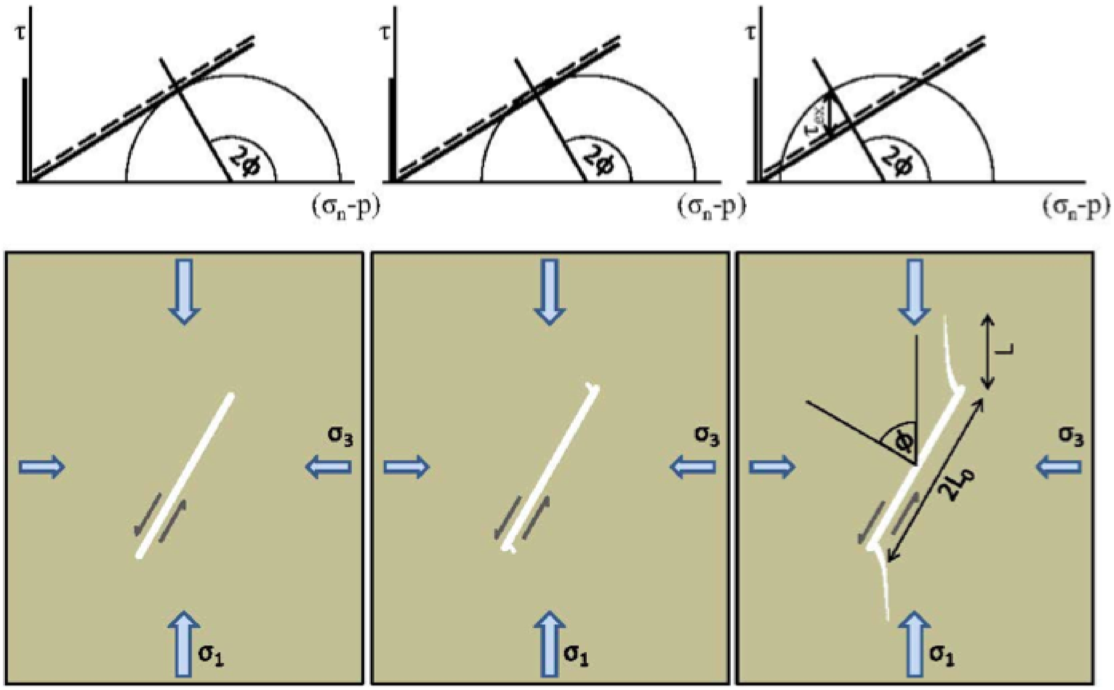

Figure 2.9: Wing-crack model, left: onset of shearing, middle: wing initiation, right: wing propagation. Image taken from Reinhard Jung[5].

new concept of fracturing should be designed, maybe using previous concept of a multi-fracture scheme. This method differs significantly from the one used by the majority of EGS projects, where long open bore holes were stimulated by pumping large amounts of water at high pressures into the well bore.

With the highly improved capacity of directional drilling and increased understanding and ability to model fracture behaviour, we wish to revisit the early concept and try to stimulate a series of parallel propagating fractures in order to achieve the desired fracture network for EGS. The idea will therefore be to drill a well parallel to the maximum principal stress and normal to the least principal stress, and stimulate parallel propagating fractures through a multi-stage fracturing job, with a goal to drill a production well above it, similar to the right illustration of figure 2.7. This approach will be followed for the rest of the thesis, and factors believed to be of key importance, as well as areas of inspiration will be discussed before a numerical approach to explore some of the found factors is described.

2.3 Dike swarms

Dike swarms are a swarm of natural magma driven hydraulic fractures that occur in the Earth's crust. Though several approaches to define dikes exists, dikes in this thesis will, in coalescence with Rivalta et al.[24], be looked at as a dike that propagates through a more or less intact rock. These dikes can propagate parallel to each other in swarms for several kilometres, and generally occur during lithospheric extension[25]. How dikes are formed, and why they grow in swarms are areas that are still coloured with some uncertainty, but our understanding of dikes and their nature has improved greatly the last years, largely due to geophysical data and to the increase in computational capacity[24]. Dikes are the biggest contributor to transport of magma in the earth's crust[24]. They occur on a large scale, and are in many places possible to observe (see figure 2.10). This can facilitate for valuable lessons, both on the geological history, but also on the nature of hydraulic fractures in the crust. Even though dikes are substantially larger in size than artificially induced hydraulic fractures, they do share some similarities. They are both fluid driven fractures, described by hydro-elastic models[24]. The nature of dikes, including their propagation and the environments in which they occur will be quickly introduced before relating it to industrial hydraulic fracturing for EGS.

Geometric properties of dikes

As the magmatic and tectonic conditions in which dikes occur differ greatly, it is only natural that some features of dikes vary. However, dikes are often in a blade-like shape with a thickness that is substantially smaller than both its length and breadth[24]. This feature can be seen in figure 2.11, which illustrates a general shape of a dike. The propagation of dikes are often normal to σ_3, though when the

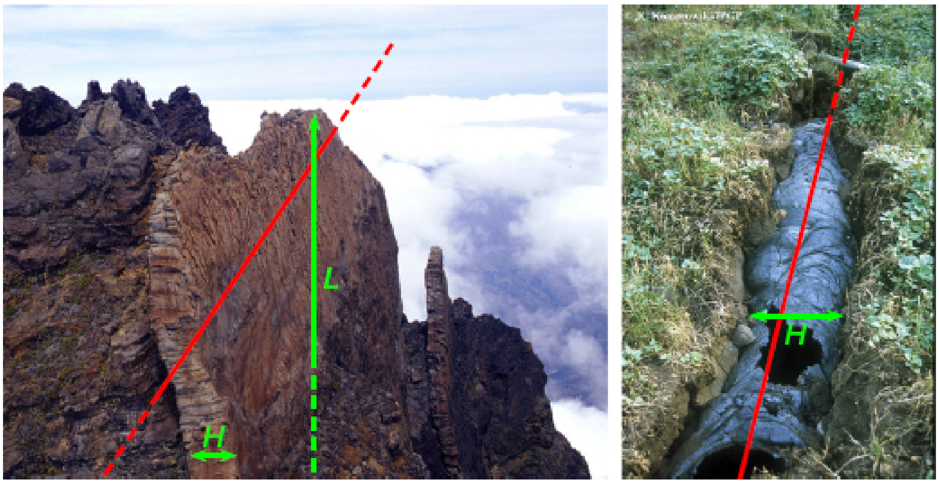

Figure 2.10: Two pictures of real life dike observations, illustrating how dikes can be observed after their formation. Image taken from Rivalta et al.[24]

minimum horizontal stress σ_h is close to the maximum horizontal stress σ_H, dikes can form radial features .

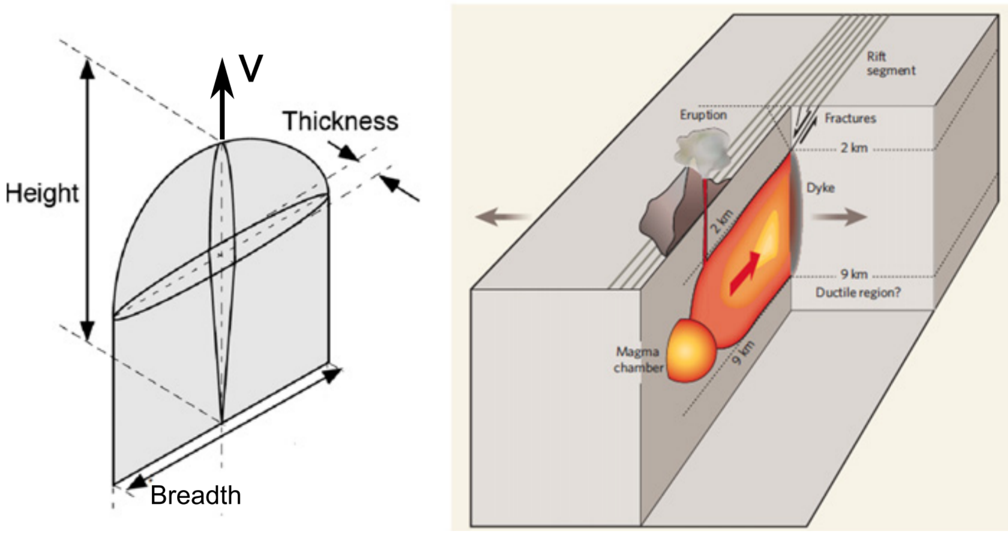

Figure 2.11: a) Vertical dike geometry, b) Dike propagation. Image taken from Rivalta et al.[24]

Knowledge and uncertainties

Over the last decades dikes have received substantial academic attention and a lot of questions regarding their dynamics, three dimensional shape, effects of the magmatic sources and effects of the external stress field, have been raised. A lot of progress has been made, and a review of the different school's approaches on modelling of dikes, their interaction with a range of external factors, and their geometrical and dynamical properties has been done by Rivalta et al[24]. There are, however, some barriers related to the mathematical complexity of the dikes and the computational capacity needed to take every factor into account. This leaves lot of blank spaces in our exact knowledge of the dikes nature and effect on its surroundings. However, with the steady increase in computational capacity some of the outstanding questions, such as 3D effects of propagation, interaction between dikes and their feeding source, incorporation of realistic magma properties etc., can be addressed [24].

Relation to industrial hydraulic fracturing

With the improved models and understanding of dikes, valuable lessons for industrial hydraulic fracturing can be made. Although the two differ in some fundamental ways, they do share some important similarities that can provide valuable lessons for both disciplines. Table 2.1 illustrates the similarities and differences between dikes and industrial hydraulic fractures.

Table 2.1: Similarities and differences between diking and industrial hydraulic fracturing [24]

Differences	**Similarities**
Magma can solidify during diking, which is not a factor for industrial injection fluids	Both processes can be altered in their propagation when encountering barriers or faults
Buoyancy forces typically drive dike propagation, but not industrial fractures.	Both are fundamentally fluid driven cracks
Industrial hydraulic fracturing use fluids on several orders of magnitude less viscous	Typically modelled by similar elasto-hydro-dynamic crack propagation
Leak-offs are often substantial in industrial fracturing, but negligible in diking	Both processes induce seismicity
Dikes achieve volumes on several orders of magnitude bigger than industrial fractures	Both processes can result in a singular feature as well as a swarm or network of fluid driven cracks

Solidified dikes can be observed and mapped long after their formation, but we normally have sparse information of the boundary conditions. Industrial hydraulic fractures, on the other hand, are hard to map, but with relatively well known boundary conditions. These disciplines can therefore share knowledge and act as inspiration for further research for each other[24]. For EGS fracture networks, the ability of dikes to grow in swarms is of extra interest.

As described in the previous chapter, a model to create a network of parallel propagating fractures in the direction normal to σ_3 was proposed. Such a network is similar to that of dike swarms, only on a smaller scale. There are still many uncertainties related to the formation of dike swarms and their governing mechanics, but Bunger et al.[22] proposed a model where they showed that a preferred spacing h between the dikes exists on the order of the height H of the dike depending on the magmatic feeding source. With a constant pressure source the optimal spacing is $h \approx H$, while a constant influx source gives two candidates for optimal spacing, one where $h \approx 0.3H$, and one where $h \approx 2.5H$. As the height of the fracture is of key in order to find the optimal spacing, a three dimensional code is needed. But it provides some ways forward when approaching the problem of creating several parallel propagating fractures in a multi stage fracturing job. Some of the most obvious factors that can be explored are:

The stress regime How differences in stress contrasts affect multiple fracture interaction

Distance between induced fractures How the distance between the injection points in different stress regimes affect the overall fracture network geometry

Feeding Source How the different injection parameters such as injection rate, injection pressure, and the fluid viscosity affect the fracture behaviour.

It will therefore be the focus of the experimental part of this thesis to explore the effects of some of these factors through numerical modelling.

2.4 Numerical modelling of rock behaviour

Due to the need for accurate predictions of fracture propagation, and for an improved understanding of how untouched rock mass reacts to stimulation, it is of great importance to develop a tool that can help us model and understand these processes better. Over recent years there has been a lot of development in both computational power and numerical models for approximating the behaviour of rock mechanics. There are many applicable numerical models, and each has its advantages and weaknesses. Examples of numerical models used for rock mechanic modelling include Finite Element Methods (FEM), Finite Difference Methods (FDM) and Discrete Element Methods (DEM). In general, numerical models make some assumptions in order to simplify models for rock mass behaviour efficiently. The rock mass is discretized to a mesh made up of a number of elements, either in two or three dimensions. When modelling in two dimensions, there is neither stress nor strain in the out-of-plane dimension. Therefore the elastic properties for a true 2D isotropic elastic continuum must be calculated in the numerical model [26].

The rocks dynamics are defined by the interaction between the elements and by certain boundary conditions. Rock discretization, definition of macroscopic properties of the rock as numerical input for the models, and implementation of boundary conditions all vary between numerical methods. As the scope of this thesis is to investigate the nature of propagating hydraulic fractures, and since methods based on finite elements have some constraints regarding dynamic fracture modelling, DEM is a well-suited choice. It is less computationally demanding than FEM, and has already been applied to model dynamic fracturing processes with some success [27]. One of the main challenges with the DEM model is the difficulty in calibrating the model's rock properties [28]. To overcome this limitation Alassi 2008 proposed a modification to DEM called Modified Discrete Element Method (MDEM). In this thesis MDEM will be used to model rock mechanic behaviour, and it will be coupled with a fluid mechanic model called Tough2 to dynamically model fracture initiation and propagation. One of the major benefits with MDEM is that it behaves similar to FEM before rock failure and DEM after [29]. This allows maintaining some of the benefits of FEM in addition to handling fracture propagation with ease [28]. A brief introduction to MDEM, and its relation to Tough2 will be given. For a more comprehensive review, see Alassi 2008.

MDEM

Currently MDEM is a two dimensional model where the three dimensional reservoir properties are taken as input, before the equivalent two dimensional values, for use in the model, are calculated. MDEM uses the concept of Voronoi diagrams, as exhibited in figure 2.12, to discretise the modelled rock. The mesh used is two-dimensional, and consists of a number of triangles, where each node of the triangle represents the centre of an element. With this definition each triangle represents a cluster of three elements, and contains three contact surfaces. The normal contact forces $\mathbf{f}_n$ and their relation to the relative displacements $\mathbf{u}_n$ can be defined by the internal constitutive model

$$\begin{pmatrix} f_{n1} \\ f_{n2} \\ f_{n3} \end{pmatrix} = \begin{bmatrix} k_{n1} & a_{12} & a_{13} \\ a_{21} & k_{n2} & a_{23} \\ a_{31} & a_{32} & k_{n3} \end{bmatrix} \cdot \begin{pmatrix} u_{n1} \\ u_{n2} \\ u_{n}3 \end{pmatrix}. \tag{2.3}$$

Here, k_{ni} is the normal stiffness coefficient at the contact i, and a_{ij} are the stiffness coefficients which make up the modification from the original DEM. By denoting the internal stiffness matrix $\mathbf{K}$, (2.3) can be written on the form

$$\mathbf{f_n} = \mathbf{K} \cdot \mathbf{u_n}. \tag{2.4}$$

The matrix $\mathbf{K}$ can be obtained through the relation between stress and strain defined by the value of the conventional constitutive matrix $\mathbf{C}$. With stress defined as $\boldsymbol{\sigma}= (\sigma_{xx}\ \sigma_{yy}\ \sigma_{xy})^T$, and the strain as $\boldsymbol{\epsilon}=(\epsilon_{xx}\ \epsilon_{yy}\ \epsilon_{xy})^T$ we can write

$$\boldsymbol{\sigma} = \mathbf{C} \cdot \boldsymbol{\epsilon}. \tag{2.5}$$

If we denote the normal vector orientation of the contact m inside the cluster θ_m, the unit normal matix $\mathbf{M}$ is defined as

$$\mathbf{M} = \begin{bmatrix} I_{11}^2 d_1 & I_{12}^2 d_1 & I_{11} I_{12} d_1 \\ I_{21}^2 d_2 & I_{22}^2 d_2 & I_{21} I_{22} d_2 \\ I_{31}^2 d_3 & I_{32}^2 d_3 & I_{31} I_{32} d_3 \end{bmatrix}. \tag{2.6}$$

Here, $I_{m1} = \cos\theta_m$, $I_{m2} = \sin\theta_m$ and d_m is the distance between two elements. Denoting the area of a cluster A, the following then holds:

$$\boldsymbol{\sigma} = \frac{1}{A} \cdot \mathbf{M}^T \cdot \mathbf{f_n} \tag{2.7}$$

$$\mathbf{u_n} = \mathbf{M} \cdot\ \boldsymbol{\epsilon} \tag{2.8}$$

By combining equations (2.3)-(2.8) the relationship between the conventional constitutive matrix $\mathbf{C}$, the unit normal matrix $\mathbf{M}$ and the constitutive stiffness matrix $\mathbf{K}$ is

$$\mathbf{C} = \frac{1}{A} \cdot \mathbf{M}^T \cdot \mathbf{K} \cdot \mathbf{M}. \tag{2.9}$$

After calculating $\mathbf{K}$ from (2.9), the forces are applied to each element. The motion of the elements is updated by applying Newton's second law. If a cluster meets the pre-defined failure criterion, the cluster, which initially is defined as an intact cluster, is instead defined as a failing cluster. Stiffness coefficients are updated, the a_{ij} values are deleted, the clusters separate and a crack formed. After redistributing the stresses, the failing cluster is given the properties of a predefined fracture. See Alassi 2010 et al[29] for more details.

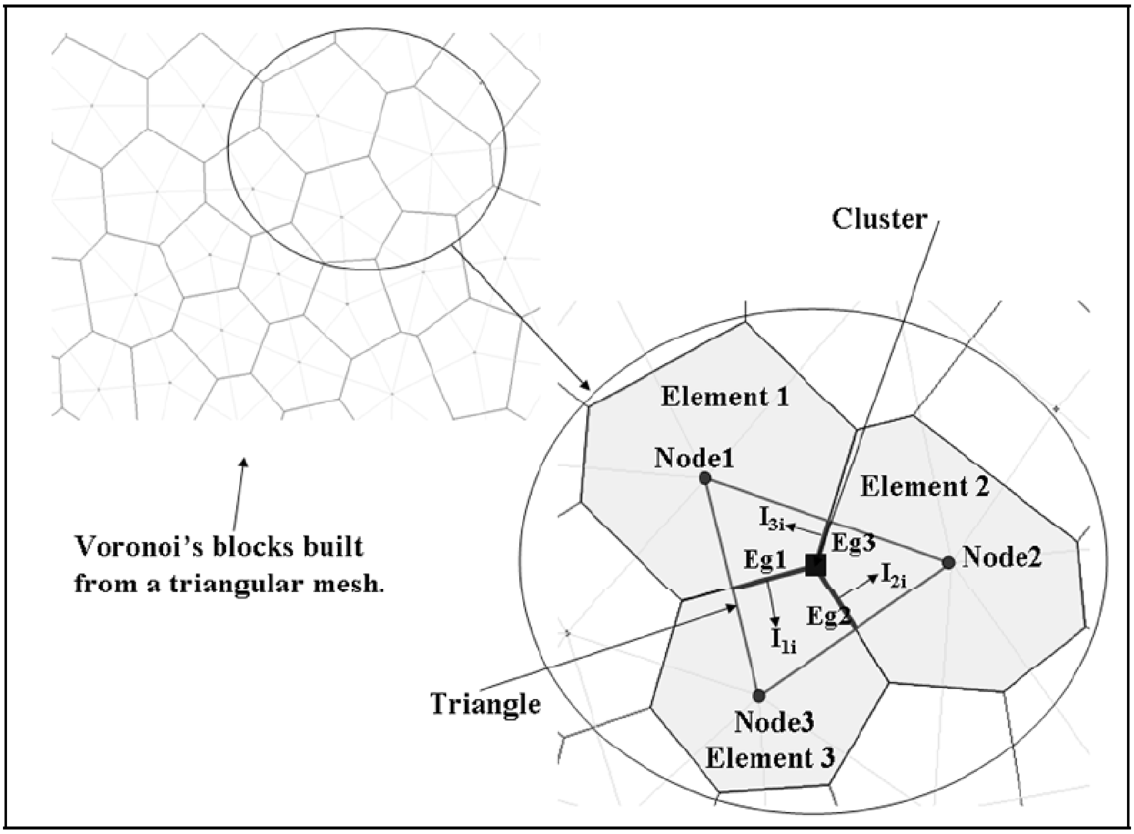

Figure 2.12: An illustration of how MDEM defines its elements, taking clusters from Voronoi's diagram. Each cluster contains three elements with three contact surfaces (Eg1, Eg2, Eg3). Image taken froms Alassi et al.[28]

Coupling with Tough2

MDEM is also coupled with a fluid flow code called Tough2. This is a general and sophisticated code, but the basic concept of how flow is defined, and the parameters exchanged between Tough2 and MDEM will be discussed here. For more details on Tough2 see Pruess[30]. Each cluster is defined as a single "fluid flow control volume". The flow, q, can be defined as the transfer of fluid from one cluster to another. This can be seen in figure 2.13, where the flow is defined from cluster A to cluster B. The flow follows Darcys Law,

$$q = \alpha \frac{k}{\mu} \frac{\Delta P}{L}, \tag{2.10}$$

where α is a permeability multiplier, k is the permeability of the rock matrix, μ is the fluid viscosity, ΔP is the pressure difference between the two clusters, and L is the distance between them. The permeability multiplier depends on the presence of cracks, and is one in the absence of cracks and larger if there are cracks present. Initially, the fracturing fluid parameters are defined and sent to Tough2. Tough2 processes the mesh to define flow paths, permeability, porosity, volume and pressures. Once Tough2 has all the information from MDEM, it starts the injection at a user-defined rate. For each time step the given volume is injected into the defined clusters, flow is calculated, and new pressures for the affected triangles are returned to MDEM. Pressures are then applied to the given triangles. MDEM runs to stabilize the model and finally an updated permeability multiplier is returned to Tough2 to continue the cycle. By repeating this loop it is possible to initiate and propagate fractures within a 2D rock mass.

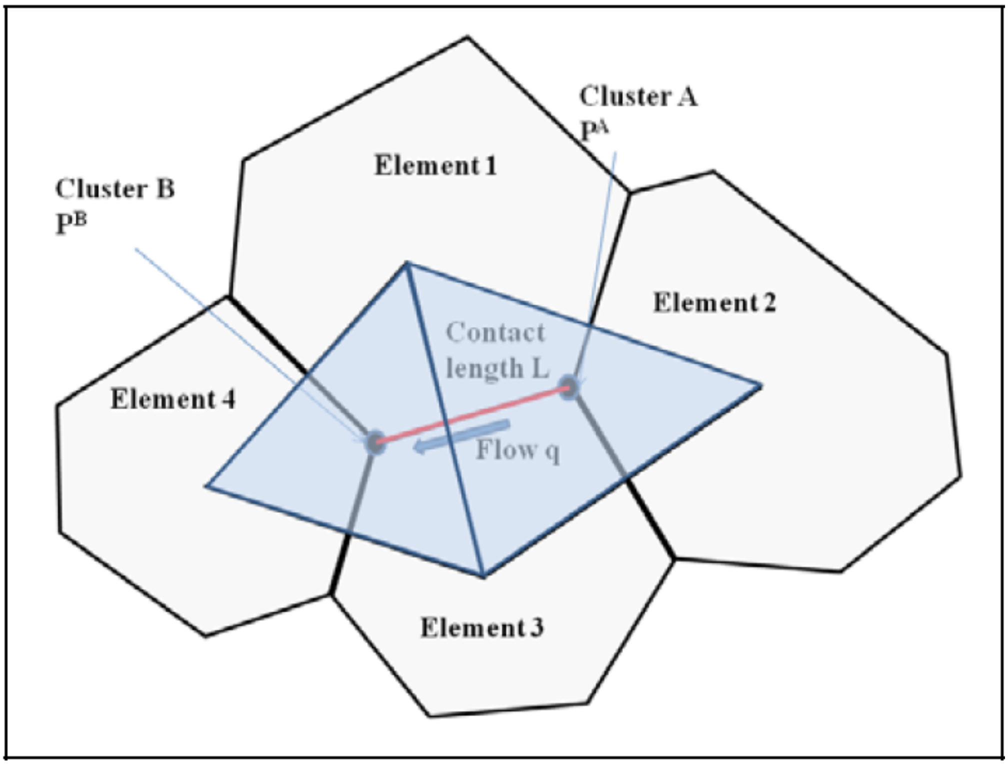

Figure 2.13: Illustration of how MDEM is coupled with Tough2. When clusters A and B fail, the flow in the modelled crack (shown in red) will be represented by a flow q, from cluster A to cluster B. Image taken from Alassi et al. [28]

Advantages and limitations

All numerical models of rock mechanics are approximations of real life situations, and will never be perfect. They can, however, come close to real behaviour, and as such be useful tools for better understanding of certain processes, thus providing accurate enough results to act as guidance when designing fracturing jobs. MDEM is well tested to model rock behaviour fairly accurately. The coupling with Tough2, allowing for dynamic modelling of fluid injection and fracture propagation, has been shown to work in a satisfactory manner[28]. With these properties it is possible to explore many of the challenges towards a successful EGS fracture network. Some of the most prominent factors for EGS that are possible to explore with MDEM/-Tough2 and some of the limitations of the version of MDEM used in this thesis are presented in table 2.2. Note that many of the limitations are possible to implement in the code, but it was not within the reach of this thesis to do it.

Table 2.2: Advantages and limitations of the MDEM version used in this thesis towards EGS fracture network investigation. Note many of the limitation points are possible to add in MDEM, but was not within the scope of this thesis to do it.

Factors that can be explored	**Limitations**
Multiple fracture interaction	The code is only available in 2D
Injection rate	Thermal effects are not included
Injection fluid viscosity	No natural discontinuities was added for this thesis's simulations.
Effect of rock parameters	A homogeneous reservoir was assumed
Effect of stress regime	No natural stress variations, fault zones etc. was applied for this thesis's simulations
Distance between injection point	

Chapter 3

Problem description and numerical scheme

3.1 System description

As described in chapter 2, a possible alternative for EGS fracture stimulation can be found by trying to create parallel propagating swarms of fractures. The goal of this numerical study is therefore to explore some of the factors of how untouched rock mass reacts to stimulation, with the focus on consequently being able to stimulate successful parallel fracture networks for EGS projects. As presented in table 2.2, there are several factors affecting fractures ability to propagate parallel to each other for great distances that can be investigated with MDEM/Tough2. The focus for this thesis will be on exploring the effects of:

- Distance between injection points
- Stress regime contrasts

To achieve this we simulate three different injection distances and three different stress regimes in a total of nine separate simulations. The physical description of the reservoir and the simulation job is given before the numerical approximation is defined.

Physical description

Reservoir

EGS reservoirs must be realized at great depths, so that high enough temperatures can be achieved at a large variation of locations across the world. This involves stimulating at depths normally in the crystalline basement. The used reservoir rock in these simulations is granite, with the properties presented in table 3.1. These values for rock properties are chosen as average values from deep well projects and former EGS research[31–36]. The hypothetical reservoir is therefore a volume of granite at depths bellow 5 km, in the crystalline basement. Even though the realistic reservoir is likely to have heterogeneity, the rock for the simulation is assumed an homogeneous and intact rock for numerical simplicity. The stress values are varied from simulation to simulation, but within a predefined viable range.

Table 3.1: Input granite material properties for MDEM, taken as average values from deep well projects and former EGS research[31–36]

Property	Value
Elastic modulus(GPa)	57.9
Poisson's ratio	0.42
Tensile Strength(MPa)	9
Cohesion (MPa)	30
Density (g/cm^3)	2560
Porosity (%)	2
Permeability (m^2)	$2 \cdot e^{-19}$

Stimulation job

It is assumed that the reservoir is penetrated by a horizontal injection well, aligned with the minimum principal stress, and normal to the maximum principal stress. The thought is therefore to drill the injection well, then attempt to stimulate vertical fractures, before drilling another production well directly above it at a certain distance. The stimulation designs that will be simulated include various point injections, which are thought to resemble an injection procedure carried out through perforations in the production casing. The number of perforations and the distance between them is varied.

Numerical description

Reservoir

A two-dimensional mesh is used to represent the rock matrix. The dimensions of the reservoir is 100m×200m and the mesh consists of approximately 72,000 elements.

This mesh, as shown in figure 3.1, has a higher density of nodes in the reservoir, and the node density decreases gradually when we move towards the boundary of the mesh. The vertical stress is applied in the y-direction and the minimum horizontal stress in the x-direction. The depth of each element is assumed 0.5 meters. Stress regimes, number of injection points and the distances between these for the different simulations are given in table 3.2.

Table 3.2: Injection parameters for all simulations. The minimum horizontal stress σ_h is 35 MPa for all simulations, σ_v is the vertical stress, I_p is the number of injection points and d_i is the distance in meters between the injection points.

Simulation no.	σ_v(MPa)	I_p	d_i(m)
1	70	3	10
2	70	5	5
3	70	9	3
4	50	3	10
5	50	5	5
6	50	9	3
7	40	3	10
8	40	5	5
9	40	9	3

Stimulation job

The horizontal injection well of our reservoir is assumed drilled along the x-axis, and therefore all the stimulation points are on this axis. An example of which elements are used for injection with five injection points is shown in figure 3.2. Tough2 simulates the injection procedure with the injection parameters defined in table 3.3. The multiple injection points for each system receive the exact same injection procedure, and is injected in a parallel process. This means that the rate is assumed given evenly in the borehole, and each point receives the rate, divided by number of injection points.

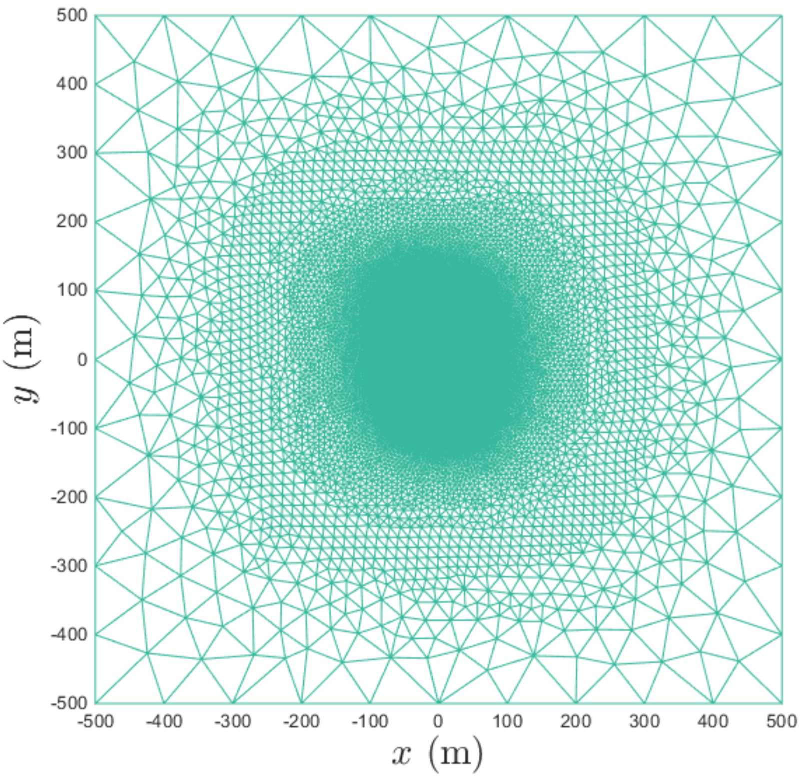

Figure 3.1: Illustration of the mesh used to represent the reservoir in the numerical simulations of this thesis

Table 3.3: Input injection parameters for Tough2

Property	Value
Volume of a triangle in injection zone (m^3)	0.0625
Injection fluid	Water
Initial Injection rate (m^3/s)	0.065

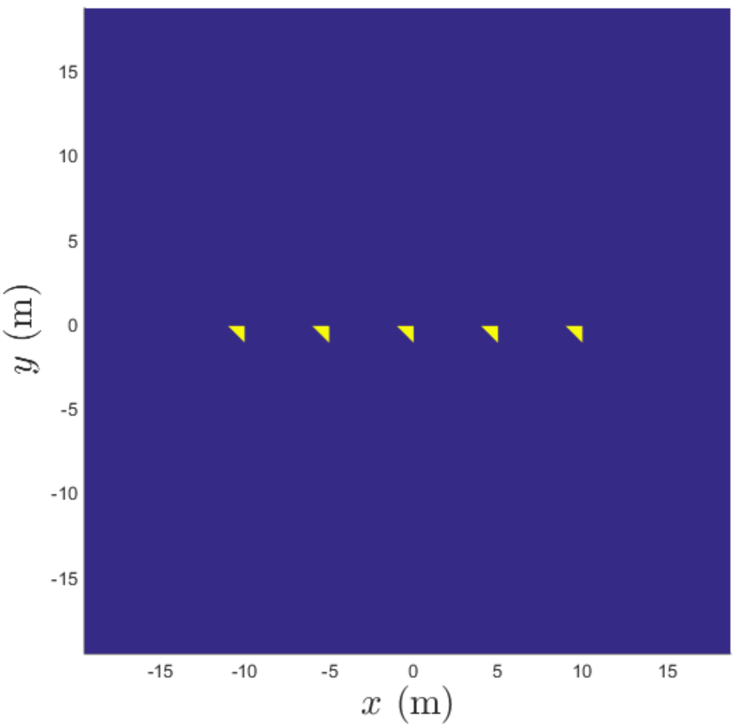

Figure 3.2: Illustration of elements that are used for injection. This is a case with five injection points with five meters in-between.

Chapter 4

Results

In this chapter the results of the nine simulations presented in table 3.2 will be given. Each simulation's fracture propagation growth is given by 6 plots at spread out time steps. For a more detailed view with higher resolution and more frames of the fracture growth, see the attached movies (if not available contact author for the movie files). The file names are as given: xstress_I_p_σ_v_σ_h. In figure 4.10 the different simulations maximum fracture distance from the well is plotted versus the time of injection.

4.1 Fracture growth plots

In this section plots of fracture propagation with stress-shadowing effects in the x-direction are illustrated. The green elements are fractures. Otherwise the colors represents the value of x-stress as given on the colorbar. For a more detailed view of stress shadowing effect see movie files.

Simulation 1

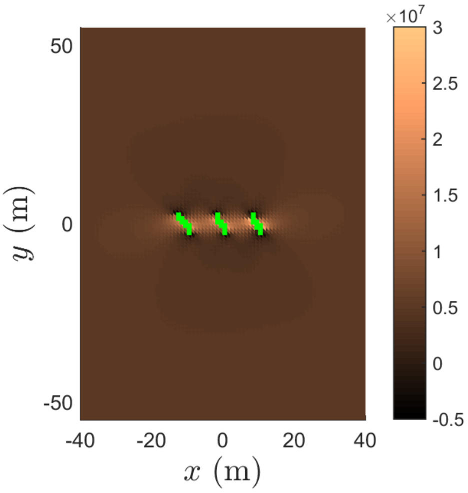

(a) injection time(s) = 185

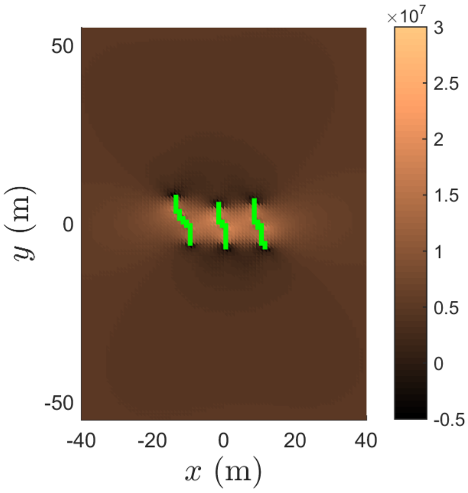

(b) injection time(s) = 385

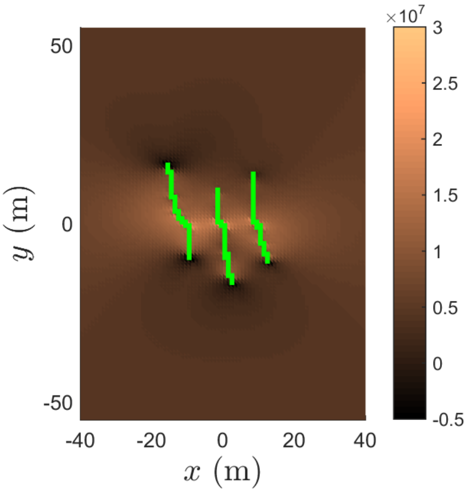

(c) injection time(s) = 585

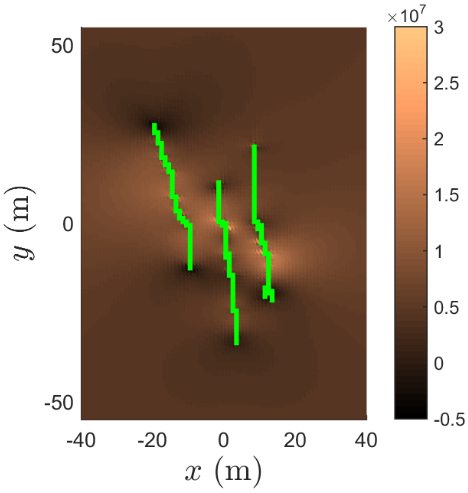

(d) injection time(s) = 725

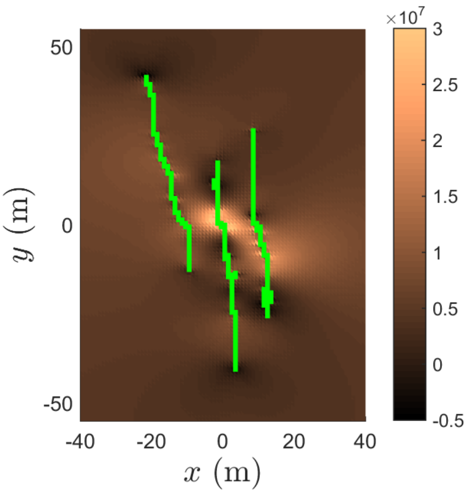

(e) injection time(s) = 920

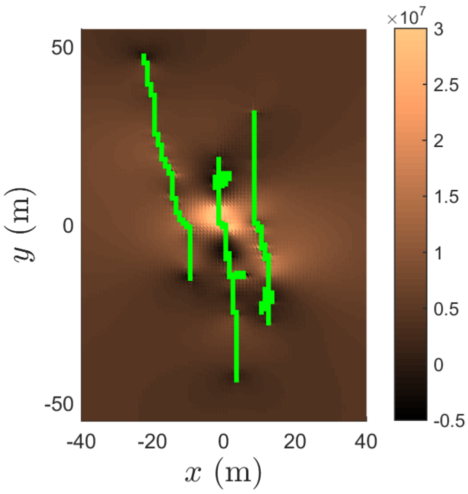

(f) injection time(s) = 990

Figure 4.1: Simulation with injection in 3 points at 10 meters apart, with σ_v=70 MPa and σ_h=35 MPa. Plot of fracture propagation with stress in x-direction (MPa). The green elements are fractures. Otherwise the colors represents the value of x-stress as given on the colorbar.

Simulation 2

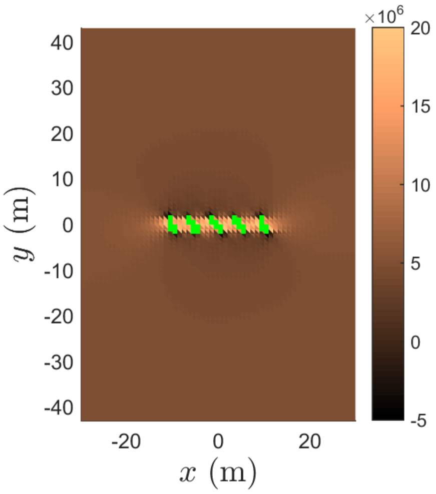

(a) injection time(s) = 285

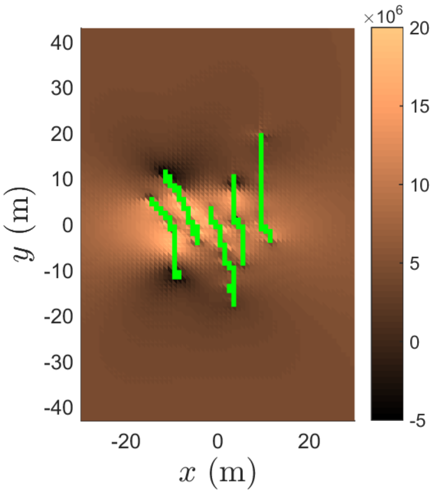

(b) injection time(s) = 705

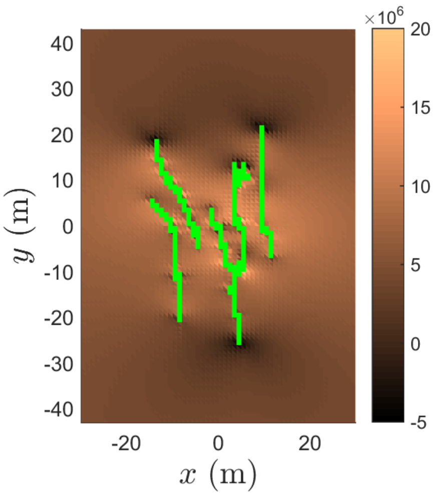

(c) injection time(s) = 821

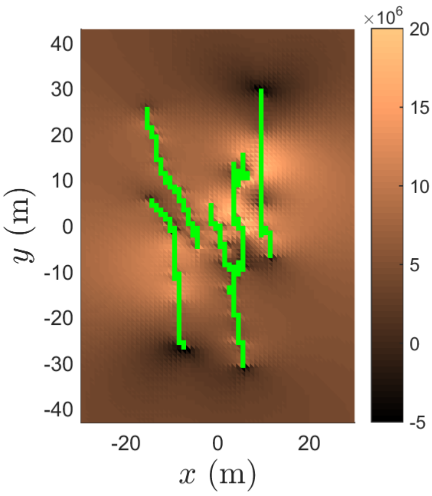

(d) injection time(s) = 951

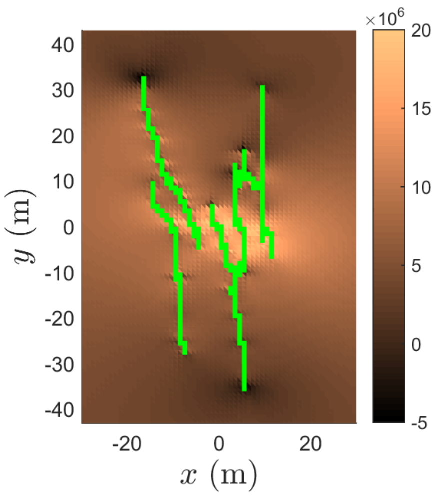

(e) injection time(s) = 1081

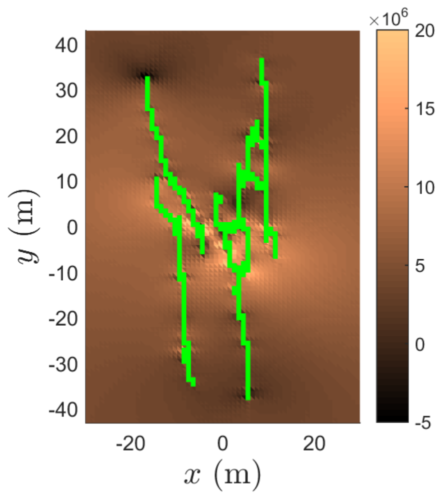

(f) injection time(s) = 1111

Figure 4.2: Simulation with injection in 5 points at 5 meters apart, with σ_v=70 MPa and σ_h=35 MPa. Plot of fracture propagation with stress in x-direction (MPa). The green elements are fractures. Otherwise the colors represents the value of x-stress as given on the colorbar.

Simulation 3

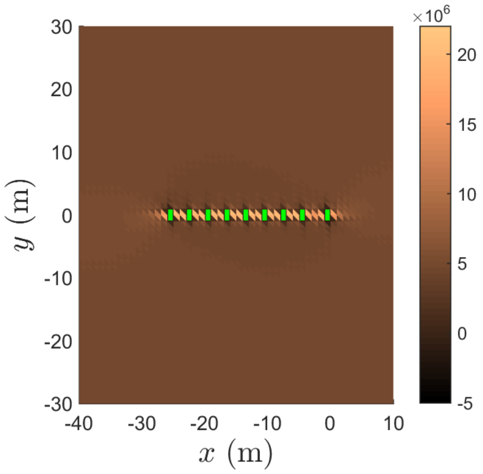

(a) injection time(s) = 345

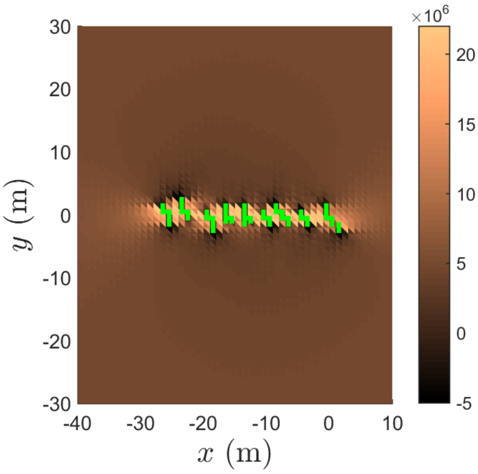

(b) injection time(s) = 985

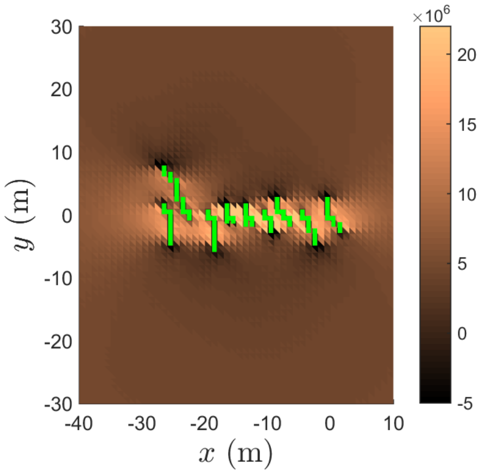

(c) injection time(s) = 1285

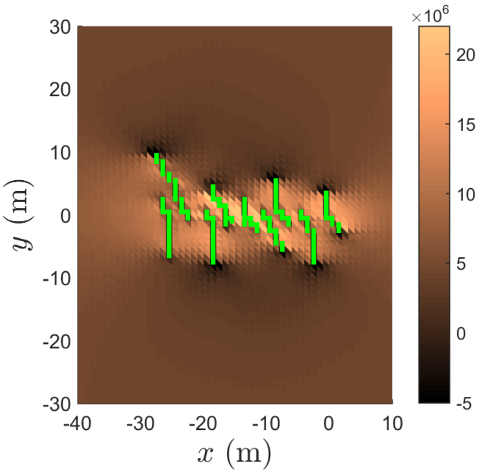

(d) injection time(s) = 1525

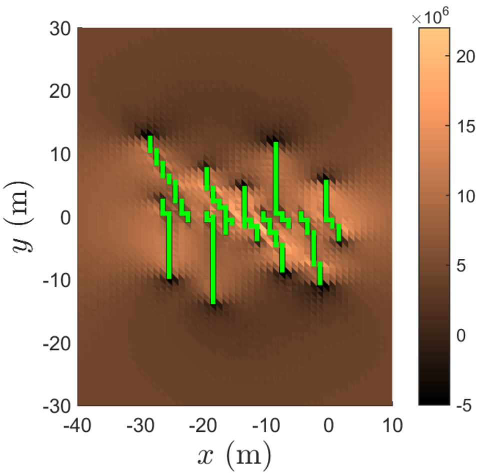

(e) injection time(s) = 1785

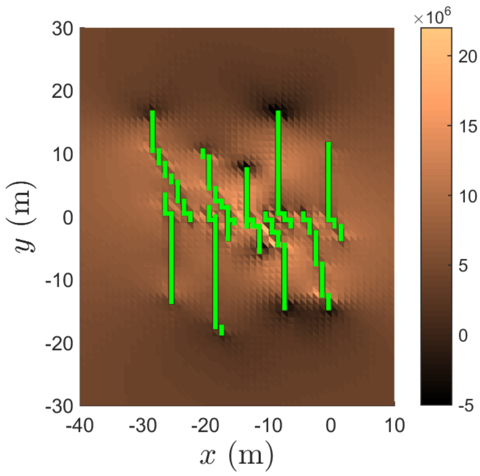

(f) injection time(s) = 2045

Figure 4.3: Simulation with injection in 9 points at 3 meters apart, with σ_v=70 MPa and σ_h=35 MPa. Plot of fracture propagation with stress in x-direction (MPa). The green elements are fractures. Otherwise the colors represents the value of x-stress as given on the colorbar.

Simulation 4

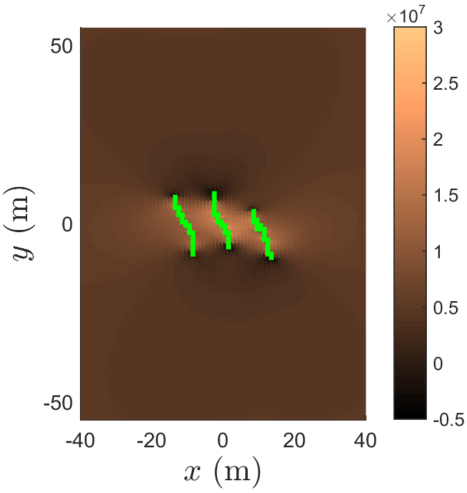

(a) injection time (s) =20

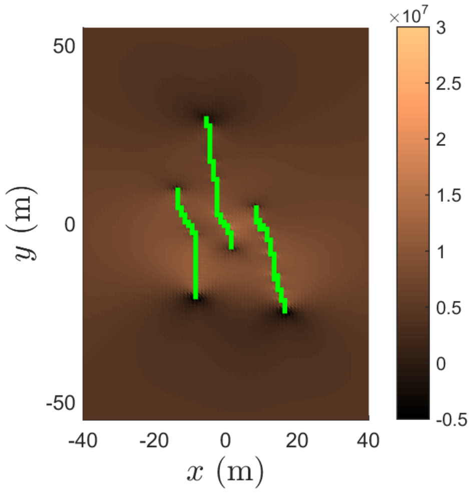

(b) injection time(s) = 320

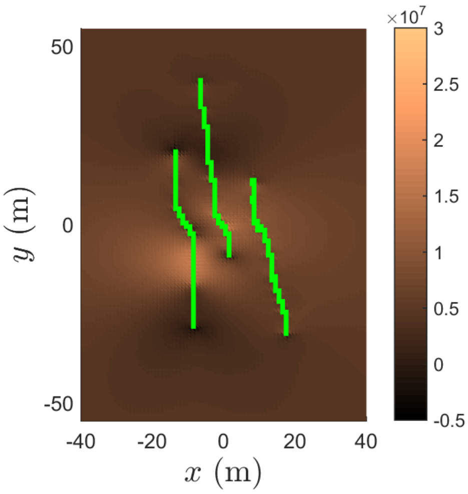

(c) injection time(s) = 425

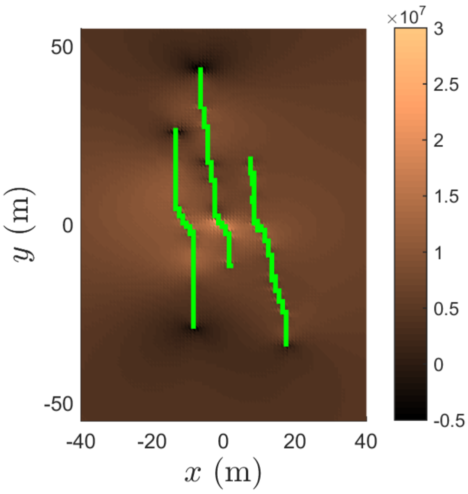

(d) injection time(s) = 525

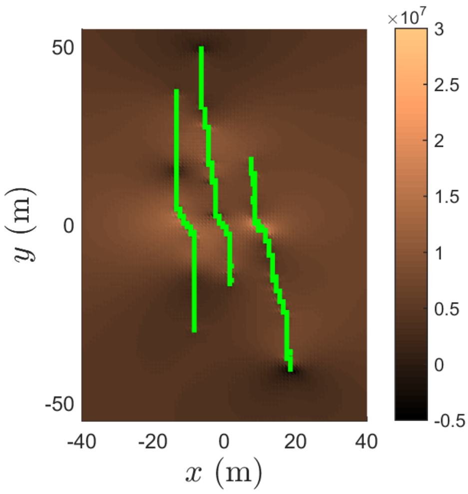

(e) injection time(s) = 605

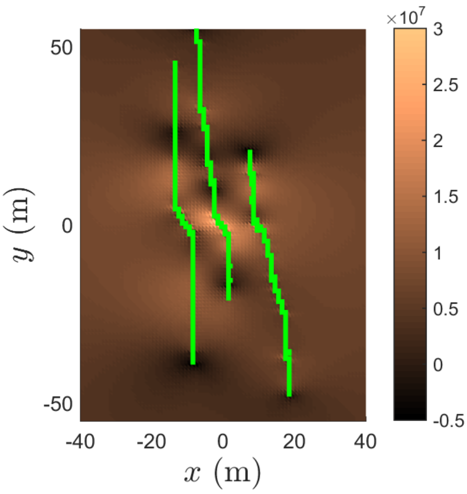

(f) injection time(s) = 700

Figure 4.4: Simulation with injection in 3 points at 10 meters apart, with σ_v=50 MPa and σ_h=35 MPa. Plot of fracture propagation with stress in x-direction (MPa). The green elements are fractures. Otherwise the colors represents the value of x-stress as given on the colorbar.

Simulation 5

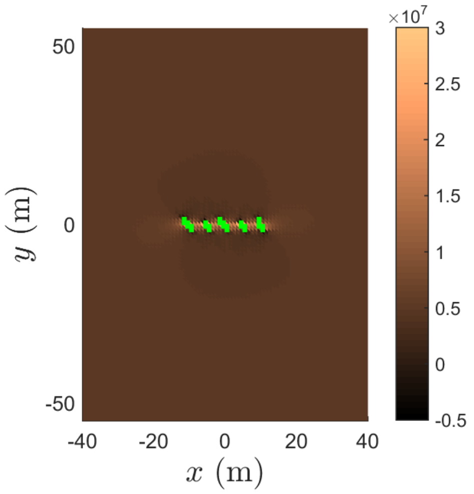

(a) injection time(s) = 165

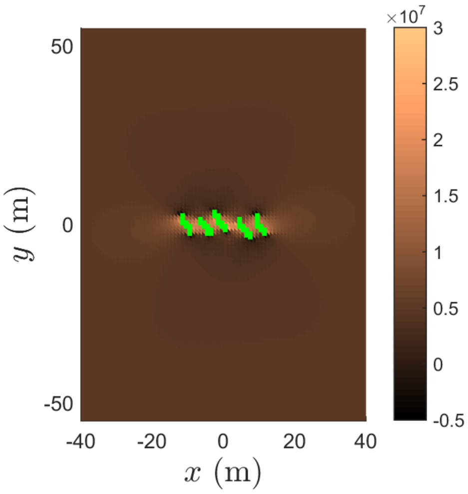

(b) injection time(s) = 345

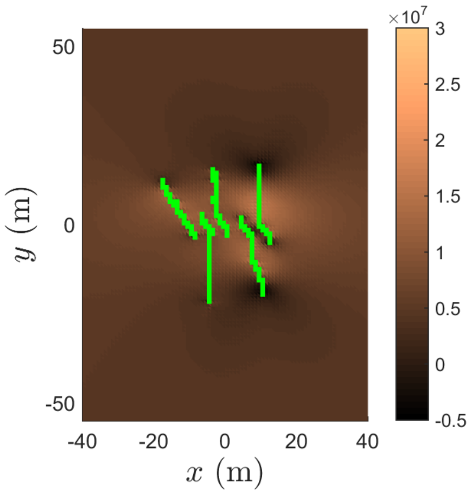

(c) injection time(s) = 645

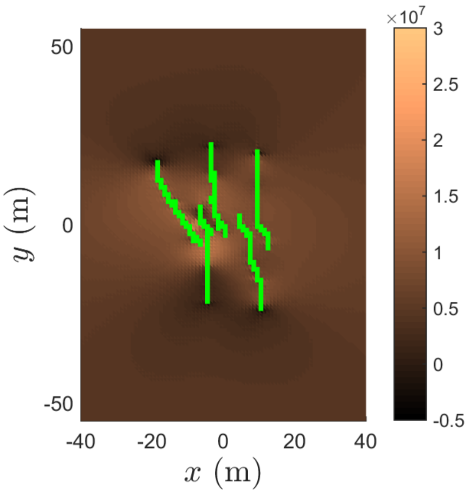

(d) injection time(s) = 722

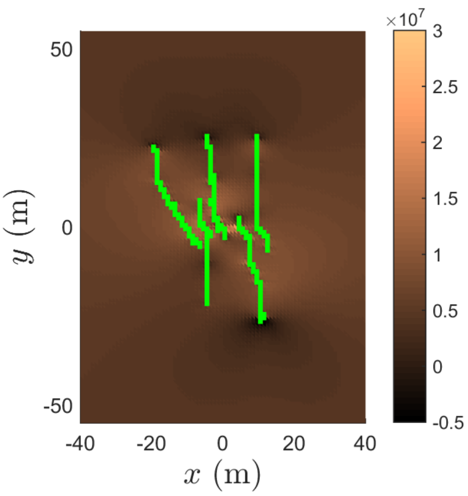

(e) injection time(s) = 827

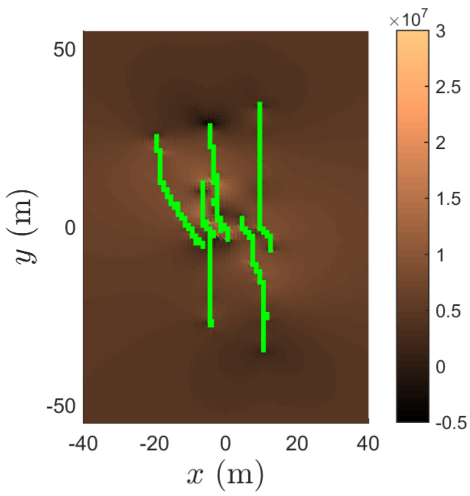

(f) injection time(s) = 947

Figure 4.5: Simulation with injection in 5 points at 5 meters apart, with σ_v=50 MPa and σ_h=35 MPa. Plot of fracture propagation with stress in x-direction (MPa). The green elements are fractures. Otherwise the colors represents the value of x-stress as given on the colorbar.

Simulation 6

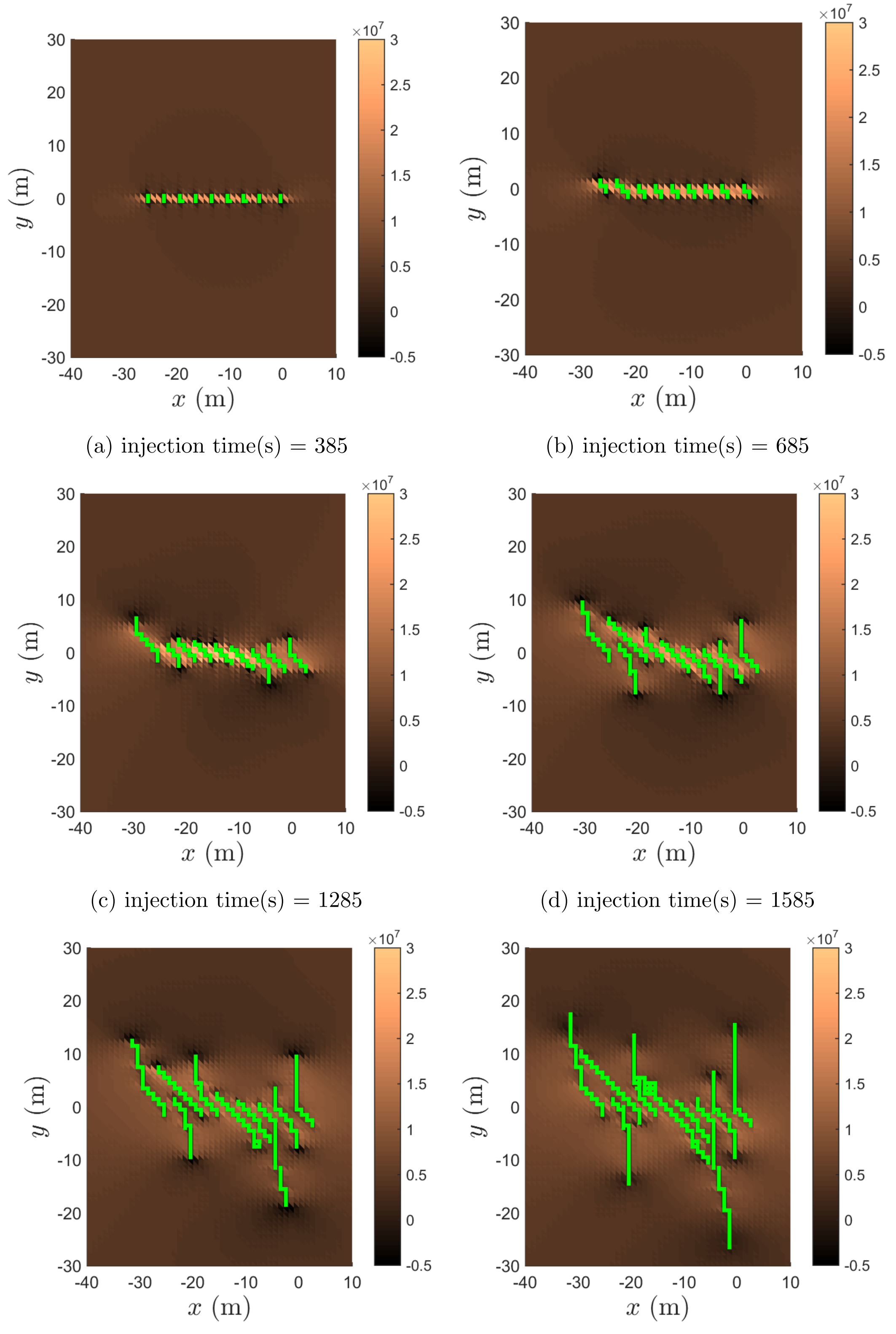

(a) injection time(s) = 385

(b) injection time(s) = 685

(c) injection time(s) = 1285

(d) injection time(s) = 1585

(e) injection time(s) = 1885

(f) injection time(s) = 2045

Figure 4.6: Simulation with injection in 9 points at 3 meters apart, with σ_v=50 MPa and σ_h=35 MPa. Plot of fracture propagation with stress in x-direction (MPa). The green elements are fractures. Otherwise the colors represents the value of x-stress as given on the colorbar.

Simulation 7

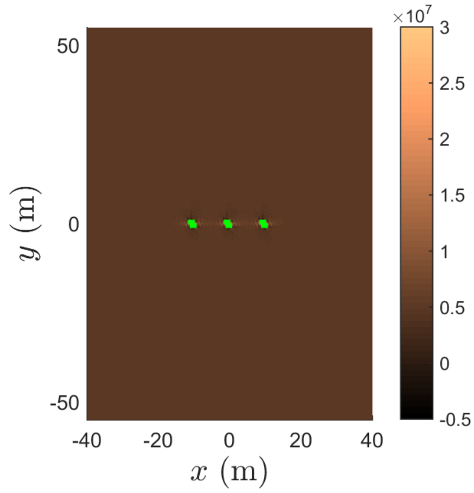

(a) injection time(s) = 45

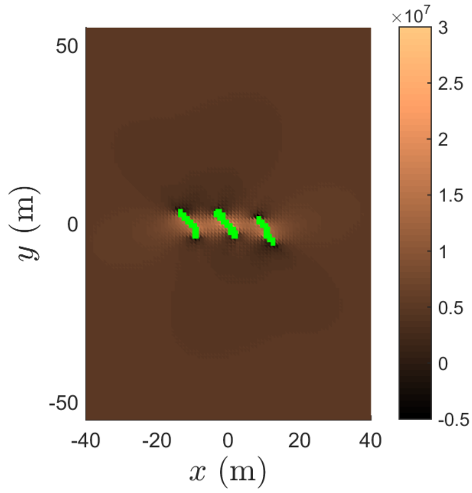

(b) injection time(s) = 225

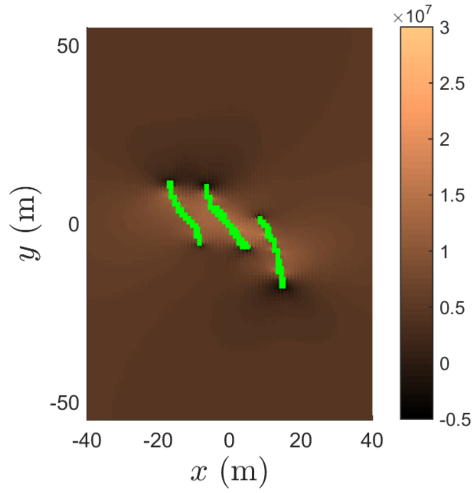

(c) injection time(s) = 325

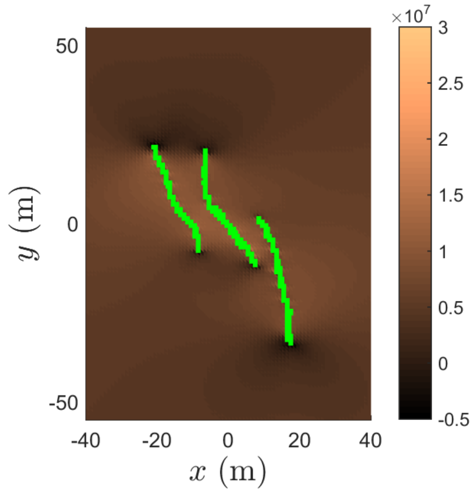

(d) injection time(s) = 625

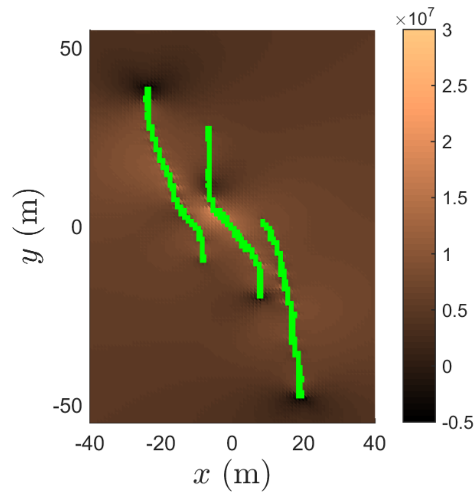

(e) injection time(s) = 825

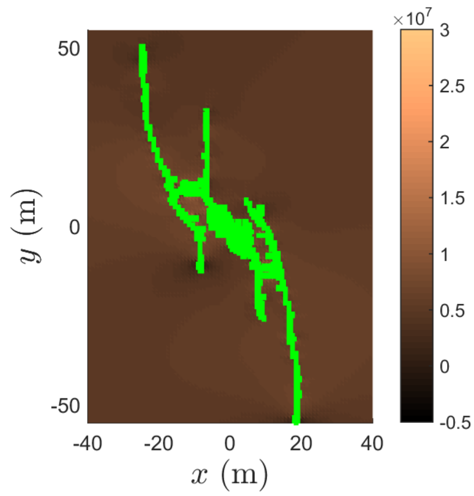

(f) injection time(s) = 892

Figure 4.7: Simulation with injection in 3 points at 10 meters apart, with σ_v=40 MPa and σ_h=35 MPa.Plot of fracture propagation with stress in x-direction (MPa). The green elements are fractures. Otherwise the colors represents the value of x-stress as given on the colorbar.

Simulation 8

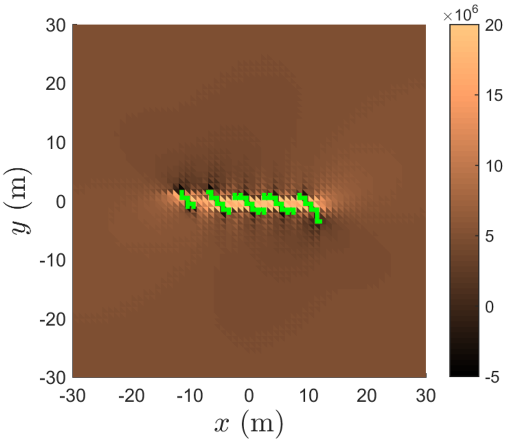

(a) injection time(s) = 205

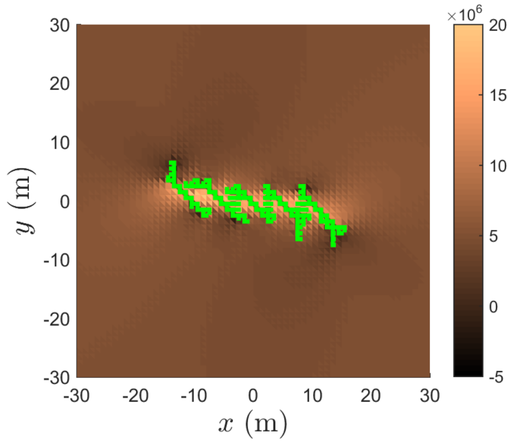

(b) injection time(s) = 310

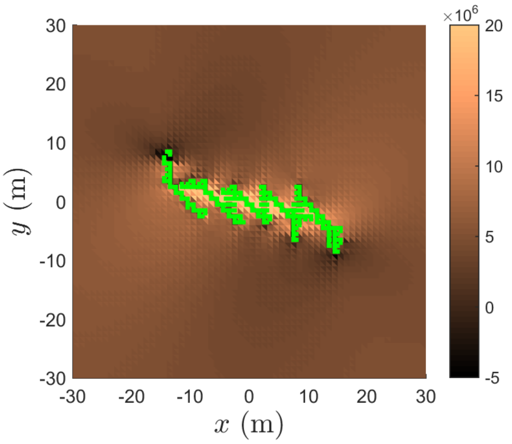

(c) injection time(s) = 430

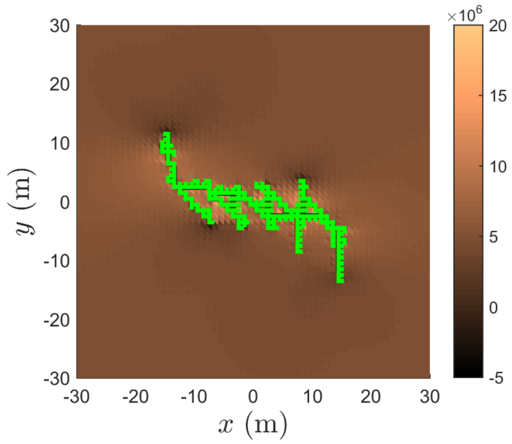

(d) injection time(s) = 547

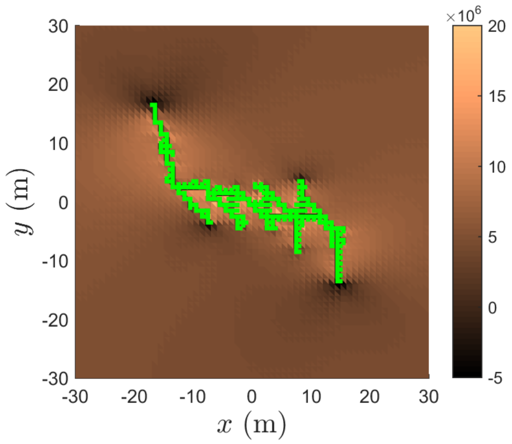

(e) injection time(s) = 657

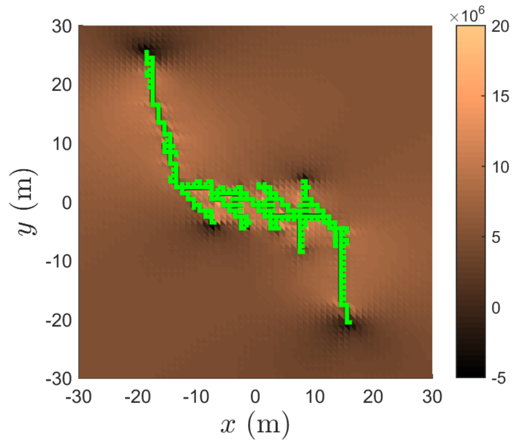

(f) injection time(s) = 737

Figure 4.8: Simulation with injection in 5 points at 5 meters apart, with σ_v=40 MPa and σ_h=35 MPa. Plot of fracture propagation with stress in x-direction (MPa). The green elements are fractures. Otherwise the colors represents the value of x-stress as given on the colorbar.

Simulation 9

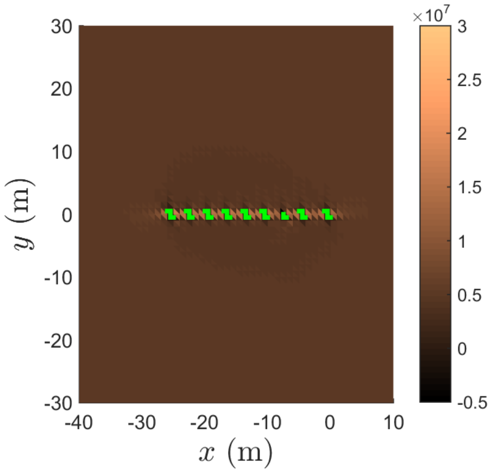

(a) injection time(s) = 225

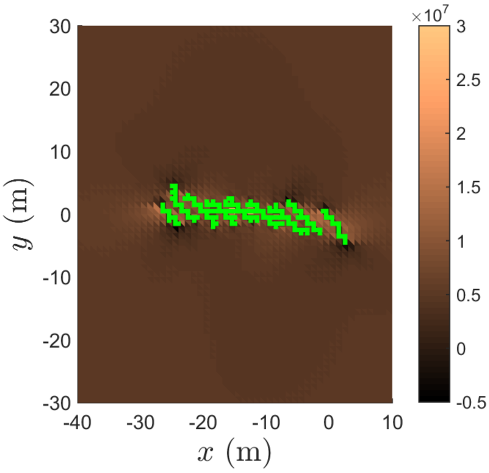

(b) injection time(s) = 705

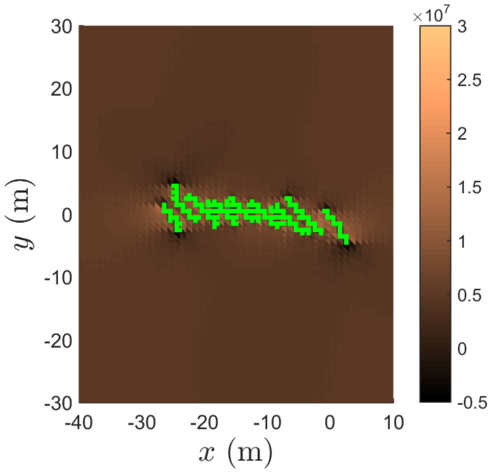

(c) injection time(s) = 820

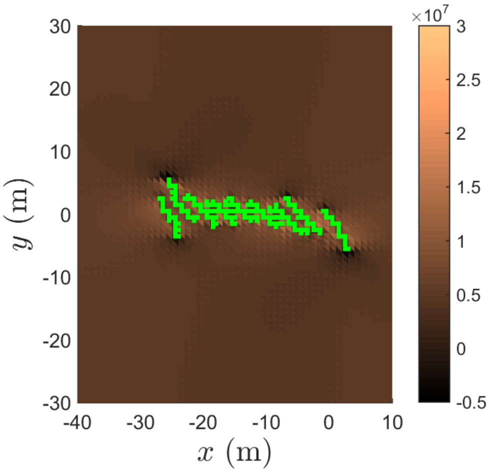

(d) injection time(s) = 950

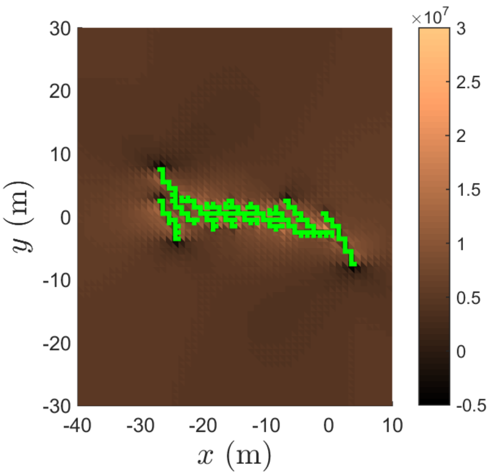

(e) injection time(s) = 1070

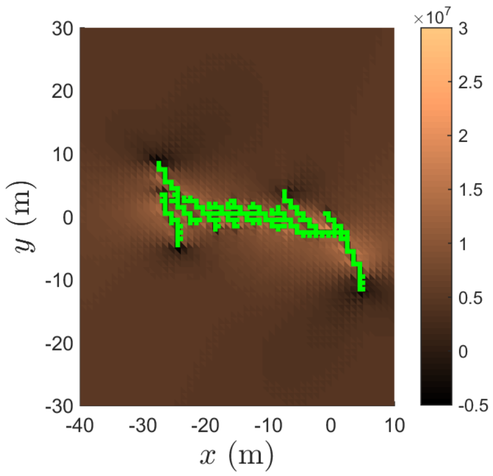

(f) injection time(s) = 1190

Figure 4.9: Simulation with injection in 9 points at 3 meters apart, with σ_v=40 MPa and σ_h=35 MPa. Plot of fracture propagation with stress in x-direction (MPa). The green elements are fractures. Otherwise the colors represents the value of x-stress as given on the colorbar.

4.2 Maximum fracture length

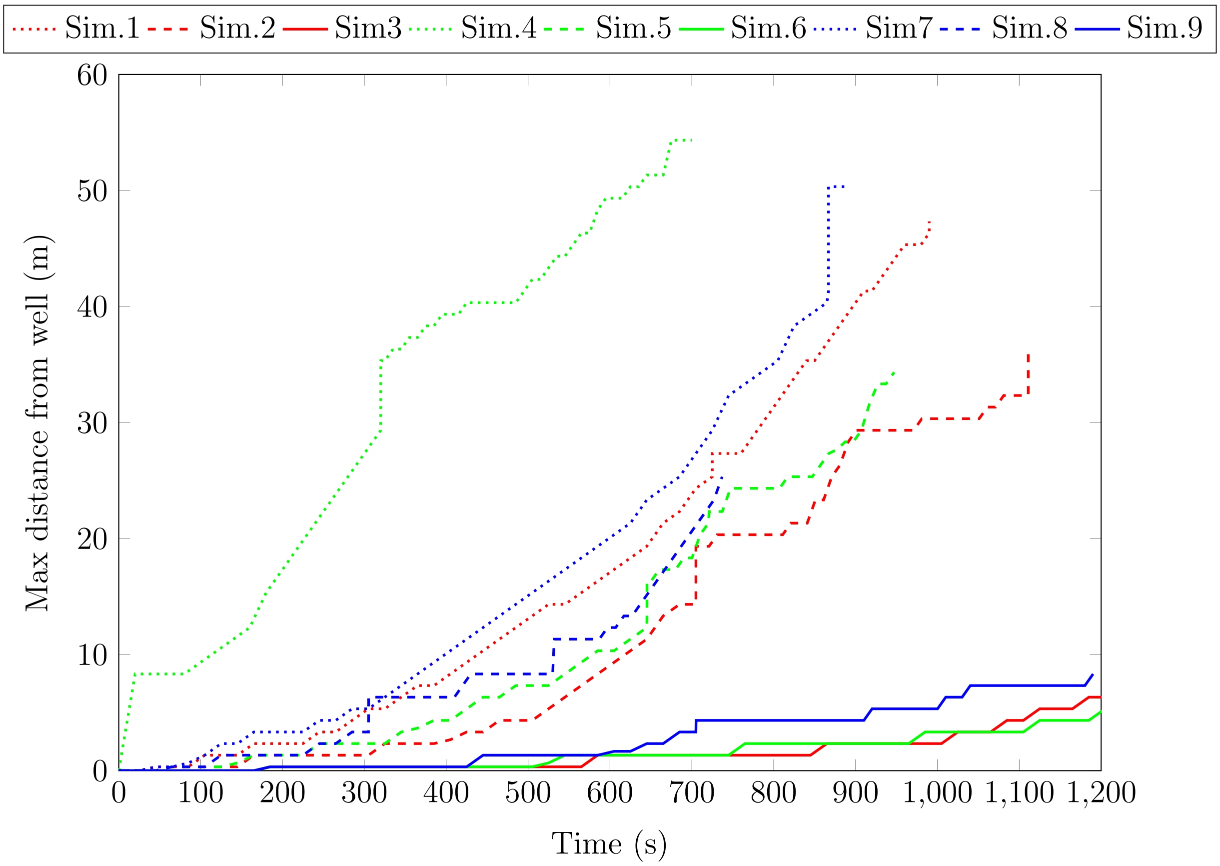

Figure 4.10: Plot of the maximum fracture distance from the borehole vs. time of injection. On the legend Sim. is used as abbreviation from simulation. See table 3.2 for simulation details. The color refers to the different stress regimes, and the line style refers to the different distances between injection points

Chapter 5

Discussion

5.1 Multiple fracture interaction: observations

From the fracture propagation plots (figure 4.1-4.9) it is evident that the fractures interact and affect each other's propagation. This is true regardless of distances between injection points d_i and for all stress regimes investigated. The fractures limit each other's growth, cause deviations from straight vertical fractures, and in some cases merge together. For the two more anisotropic stress regimes (σ_v=50 MPa and σ_v=70 MPa), all simulations create a series of parallel fractures, in both positive and negative y-direction. It can be seen in figures 4.1-4.6, that when a fracture starts to propagate it cause a stress-shadowing effect on the nearby fractures, increasing the stress in the x-direction. This makes it harder for the nearest fractures to propagate in the same direction. A trend is established in which approximately half the fractures mainly extend downwards and the other half upwards, alternating every other fracture.

In the cases where the stress contrast was smaller (σ_v=40 MPa), all three simulations, seen in figure 4.7-4.9, created a complex fracture network close to the well, connecting all fractures. This severely limits the ability to propagate parallel fractures. Simulation number 7 (see figure 4.7) started out with parallel propagating fractures, before the effect of fracture interaction became too strong and a complex fracture network close to the well was established. The created fracture geometry, with a network of connected fractures in the middle and a fracture extending from each end, slightly resembles a bi-wing fracture, (see figure 2.3). The same tendency is seen in simulations number 8 and 9. Only with the closer injection intervals, the complex network was established before a fracture at each end were extended away from the well (see figure 4.8f amd 4.9f). Due to long computational times, it was not possible to run simulation number 9 for a longer time, and the side fractures have not extended for long distances, but the tendency can still be seen at each end of the complex fracture network. Comparing the cases with a smaller stress contrast (σ_v=40 MPa) to the more anisotropic stress regimes (σ_v=50 MPa and σ_v=70 MPa), there is a clear difference in the ability to stimulate parallel fractures for all d_i. This indicates that with a smaller stress contrast it is easier for a complex fracture network close to the well to be established, severely limiting parallel fracture propagation.

The maximum fracture distance from the well vs. time of injection, for the different simulations is illustrated in figure 4.10. It is evident that the simulation cases with d_i=5 and d_i=10 meters between injection points, have a much steeper slope than the ones with d_i=3. The plot in figure 4.10 does not take into account the number of fractures at the maximum length, but by looking at the propagation plots it can be seen that simulations 1-6 have a number of parallel fractures at the approximately same length, but with about half the fractures in each y-direction. For simulations 7-9, however, there is mainly only one fracture in each direction able to extend far away from the well.

The distance between injection points seems to have an effect on the ability of the fractures to propagate for long distances. This factor does not appear to be linear with injection point distance, as the effect between d_i=3 to d_i=5 is much more clear than between d_i=5 and d_i=10 meters. The same is true for the effect of the stress regime. There seems to be less difference comparing σ_v=70 MPa to σ_v=50 MPa, than comparing σ_v=50 MPa and σ_v=40 MPa. In other words, the nature of the fracture network geometry is more similar in the two more anisotropic conditions, and differs completely in the condition with less stress contrast. This implies that the effect of fracture interaction is both dependent on the distance between the fractures and on the stress contrast, and that the degree of effect is not linear to either the distance nor the stress contrast.

5.2 The importance for EGS

The numerical results show that it is possible to create parallel propagating fractures, even at quite short intervals. However, the fractures only propagated to a maximum of 55 meters away from the well, and only did so in the cases with three injection points. In addition, it proved a lot harder to stimulate parallel fractures in conditions with little stress contrasts. For EGS fracture networks it is desirable to have as many fractures as close to each other as possible, propagating for long distances. These results do not illustrate what happens at the later phases of the injection job, and whether the fractures are able to propagate for distances demanded by EGS networks. But it is a start for further study, and clearly illustrates the importance of the stress regime when deciding the properties of a multi-stage fracturing job.

5.3 Uncertainties

For the simulations conducted in this thesis many simplifications were made (see table 2.2). As concluded in chapter 2, recent research shows that secondary effects must be taken into account for accurate modelling of hydraulic fractures. However, it is important to start with some simplifications to get a view of how the governing factors work. The effect of natural permeability and rock heterogeneity might have an impact on the degree with which fractures interact, implying a different optimal distance between injection points. The effect of injection parameters was not taken into account and might be capable of affecting the multiple fracture interaction. With more elements used for injection each element receives less injection rate. This was not taken accounted for in the plot in figure 4.10. This is because fractures may merge, and a fracture is not necessarily driven by the injection rate of only one element.

Chapter 6

Proposed further work

One of the focuses of this thesis was to identify factors of hydraulic fracturing important to investigate, in relation to EGS. In addition, a numerical study was carried out on two of the factors identified. For further studies, it is proposed to do numerical studies on the other factors identified in section 2.3, as well as improve the numerical code used for the simulations. Specifically, it is suggested that the following steps are taken:

Feeding source Investigate the effects variations in the feeding source will have on the fracture propagation, including:

- Injection rate
- Injection pressures
- Injection fluid viscosity

Improve MDEM Add factors of importance and improve the version of MDEM used in the thesis by adding the following effects:

- Natural discontinuities
- Heterogeneity in rock properties
- Stress zones
- Thermal effects
- Three dimensional model

Run more simulations Continue the work of this thesis by doing more simulations, at different different injection point distances and different stress regimes.

Multi-stage fracture simulations As the stress shadowing caused by the propagating fractures varied during injection, and the final value was not necessarily the maximum, an injection in series might provide different fracture network geometry. So further work should investigate the difference between injection in series and parallel, and potentially a combination between the two.

Open-borehole simulations For this thesis only point injection was done. It would be interesting to do injection simulations in an open bore hole with many borewall weaknesses.

Limit downward fracture propagation For EGS the goal is to create communication with another well, and it is not necessary to propagate fractures downwards. About half the fractures in this thesis simulations propagated downwards, so an effort to limit or deny downward fracture propagation should be done. Adding the effect of gravity will limit downward fracture propagation, and it is also possible to put a thin layer of infinitely strong elements right under the bore hole (representing a production casing or similar).

Fracture dynamics in the late phase of the fracturing job Run simulations on a larger scale and on longer time intervals do find out how long the fractures can propagate, and how the dynamics of the late phase of the fracturing job behaves.

Chapter 7

Conclusion

In order to make geothermal energy and EGS a serious alternative as a global base load power source, there is a need to consistently being able to stimulate sufficient fracture networks. Stimulating a swarm of parallel propagating fractures has been identified as a way forward for effective EGS fracture networks. By investigating properties that affect fractures propagation and ability to grow in swarms, methods to consequently stimulate sufficient fracture networks for EGS can be achieved. Dike swarms is an area of interest that can provide valuable information for the hydraulic fracture industry as our knowledge of them increase. Simulations using MDEM and Tough2 have successfully been run with a variation of stress regimes and injection point distributions. The numerical study from this thesis shows the importance of the stress regime on multiple-fracture interaction, and the need to investigate it further for accurate implementation in stimulation models. The degree at which the fractures interact are not linear to neither the stress nor the injection point distances. With small stress contrasts, there is little ability to propagate parallel fractures at short injection intervals. For further work it is important to take account of natural discontinuities, rock heterogeneity and reservoir properties that might affect fracture interaction. In addition, a variation of injection parameters has been introduced as factors of potential importance and should be included in future research and simulations.

Bibliography

[1] Solomon Susan. *Climate change 2007-the physical science basis: Working group I contribution to the fourth assessment report of the IPCC*, volume 4. Cambridge University Press, 2007.

[2] Jefferson W Tester, B Anderson, A Batchelor, D Blackwell, R DiPippo, E Drake, J Garnish, B Livesay, MC Moore, and K Nichols. The future of geothermal energy: Impact of enhanced geothermal systems (egs) on the united states in the 21st century. *Massachusetts Institute of Technology*, 2006.

[3] Mats Rongved. Geothermal energy: A literature review with a focus on identifying challenges related to the petroleum industry. Specialization project report, 2013.

[4] Enrico Barbier. Geothermal energy technology and current status: an overview. *Renewable and Sustainable Energy Reviews*, 6(1):3–65, 2002.

[5] Reinhard Jung. Egs–goodbye or back to the future. *Effective and Sustainable Hydraulic Fracturing*, pages 95–121, 2013.

[6] John L Gidley. Recent advances in hydraulic fracturing. 1989.

[7] Maurice B Dusseaul. Rock mechanics aspects of hydraulic fracturing.

[8] Erling Fjar, Rachel M Holt, AM Raaen, Rasmus Risnes, and P Horsrud. *Petroleum related rock mechanics*, volume 53. Elsevier, 2008.

[9] Peter Valkó and Michael J Economides. *Hydraulic fracture mechanics*. Wiley New York, NY, 1995.

[10] Xi Zhang, RG Jeffrey, AP Bunger, and Marc Thiercelin. Initiation and growth of a hydraulic fracture from a circular wellbore. *International Journal of Rock Mechanics and Mining Sciences*, 48(6):984–995, 2011.

[11] WW Aud, TB Wright, CL Cipolla, JD Harkrider, et al. The effect of viscosity on near-wellbore tortuosity and premature screenouts. In *SPE annual technical conference and exhibition*. Society of Petroleum Engineers, 1994.

[12] JF Manrique, A Venkitaraman, et al. Oriented fracturing-a practical technique for production optimization. In *SPE Annual Technical Conference and Exhibition*. Society of Petroleum Engineers, 2001.

[13] Hazim Hussein Abass, Mohamed Y Soliman, AM Tahini, Jim Surjaatmadja, David L Meadows, and Leopoldo Sierra. Oriented fracturing: A new technique to hydraulically fracture an openhole horizontal well. In *Proceedings SPE Annual Technical Conference and Exhibition, New Orleans, LA, USA. SPE*, volume 124483, 2009.

[14] Charles Fairhurst. Fractures and fracturing: hydraulic fracturing in jointed rock. In *ISRM International Conference for Effective and Sustainable Hydraulic Fracturing*. International Society for Rock Mechanics.

[15] TK Perkins and JA Gonzalez. The effect of thermoelastic stresses on injection well fracturing. *SPE J*, 25(1):78–88, 1985.

[16] NR Warpinski and LW Teufel. Influence of geologic discontinuities on hydraulic fracture propagation (includes associated papers 17011 and 17074). *Journal of Petroleum Technology*, 39(02):209–220, 1987.

[17] Robert G Jeffrey, Andrew Bunger, Brice Lecampion, Xi Zhang, Zuorong Chen, Andre van As, David P Allison, Willem De Beer, John Wesley Dudley, and Eduard Siebrits. Measuring hydraulic fracture growth in naturally fractured rock. In *SPE Annual Technical Conference and Exhibition*. Society of Petroleum Engineers.

[18] Roberto Suarez-Rivera, Jeff Burghardt, Sergei Stanchits, Eric Edelman, and Aniket Surdi. Understanding the effect of rock fabric on fracture complexity for improving completion design and well performance. In *IPTC 2013: International Petroleum Technology Conference*.

[19] Xi Zhang and Rob Jeffrey. Development of fracture networks through hydraulic fracture growth in naturally fractured reservoirs. In *ISRM International Conference for Effective and Sustainable Hydraulic Fracturing*. International Society for Rock Mechanics.

[20] Arash Dahi Taleghani, Milad Ahmadi, and JE Olson. Secondary fractures and their potential impacts on hydraulic fractures efficiency. In *ISRM International Conference for Effective and Sustainable Hydraulic Fracturing*. International Society for Rock Mechanics.

[21] Mikhail Geilikman, Guanshui Xu, Sau-Wai Wong, et al. Interaction of multiple hydraulic fractures in horizontal wells. In *SPE Unconventional Gas Conference and Exhibition*. Society of Petroleum Engineers, 2013.

[22] Andrew Bunger, Robert G Jeffrey, Xi Zhang, et al. Constraints on simultaneous growth of hydraulic fractures from multiple perforation clusters in horizontal wells. *SPE Journal*, 19(04):608–620, 2014.

[23] Florian Lehner and Mark Kachanov. On modelling of 'winged" cracks forming under compression. *International Journal of Fracture*, 77(4):R69–R75, 1996.

[24] E Rivalta, B Taisne, AP Bunger, and RF Katz. A review of mechanical models of dike propagation: Schools of thought, results and future directions. *Tectonophysics*, 638:1–42, 2015.

[25] Guiting Hou, Jianghai Li, Mohan Yang, Weihao Yao, Chuancheng Wang, and Yanxin Wang. Geochemical constraints on the tectonic environment of the late paleoproterozoic mafic dyke swarms in the north china craton. *Gondwana Research*, 13(1):103–116, 2008.

[26] PA Cundall, MA Ruest, AR Guest, and G Chitombo. Evaluation of schemes to improve the efficiency of a complete model of blasting and rock fracture. In Heinz Konietzky, editor, *Numerical Modeling in Micromechanics via Particle Methods: International PFC Symposium, Gelsenkirchen, Germany, 6-8 November 2002*. CRC Press, 2002.

[27] CJ De Pater, LJL Beugelsdijk, et al. Experiments and numerical simulation of hydraulic fracturing in naturally fractured rock. In *40th US rock mechanics symposium and 5th US-Canada rock mechanics symposium, American Rock Society Association*, 2005.

[28] Haitham Tayseer Alassi, Rune M Holt, Olav-magnar Nes, Srutarshi Pradhan, et al. Realistic geomechanical modeling of hydraulic fracturing in fractured reservoir rock. In *Canadian Unconventional Resources Conference*. Society of Petroleum Engineers, 2011.

[29] Haitham Alassi, Rune Holt, and Martin Landrø. Relating 4d seismics to reservoir geomechanical changes using a discrete element approach. *Geophysical prospecting*, 58(4):657–668, 2010.

[30] Karsten Pruess. Tough2: A general-purpose numerical simulator for multiphase fluid and heat flow. 1991.

[31] Luke P Frash, Marte Gutierrez, Jesse Hampton, and John Hood. Laboratory simulation of binary and triple well egs in large granite blocks using ae events for drilling guidance. *Geothermics*, 55:1–15, 2015.

[32] AV Zharikov, VM Vitovtova, VM Shmonov, and AA Grafchikov. Permeability of the rocks from the kola superdeep borehole at high temperature and pressure: implication to fluid dynamics in the continental crust. *Tectonophysics*, 370(1):177–191, 2003.

[33] Jiřina Trčková, Vladimír Šrein, Martin Št'astnỳ, and R Živor. The relationship between gneisses from the kola superdeep borehole and their surface analogues. *Acta Geodyn. Geomat*, 5(1):57–63, 2008.

[34] Felix F Gorbatsevich, Vadim L Il chenko, J Trckova, R Zivor, and Yury P Smirnov. A comparison of physical and mechanical characteristics of kola superdeep borehole core samples and their surface analogues. *ACTA GEODYNAMICA ET GEOMATERIALIA*, 1(4):85, 2004.

[35] Grímur Björbsson and Gudmundur Bodvarsson. A survey of geothermal reservoir properties. *Geothermics*, 19(1):17–27, 1990.

[36] WP Schellart. Shear test results for cohesion and friction coefficients for different granular materials: scaling implications for their usage in analogue modelling. *Tectonophysics*, 324(1):1–16, 2000.